Precision opportunities in QCD and BSM physics at the EIC

Frank Petriello

Precision QCD predictions for ep physics at the EIC

June 29, 2022

NORTHWESTERN UNIVERSITY

Argonne NATIONAL LABORATORY

Outline

- Part 1: Jet and polarized W production to NNLO in pQCD
  - Discuss the NNLO QCD corrections to inclusive jet production at the EIC, and describe the techniques used in this calculation
  - Show phenomenology of jet production at the EIC
  - Discuss the calculation of NNLO corrections to W production in polarized RHIC collisions
- Part 2: BSM probes at the EIC
  - Introduce the Standard Model Effective Field Theory (SMEFT) framework for future new physics searches at the LHC, EIC and elsewhere
  - Show that the EIC has an important role to play in resolving LHC blind spots in the SMEFT parameter space, due to its high luminosity, low systematic errors, and ability to polarize beams

The EIC is a precision machine

- The EIC will study the SM in ways not possible with current machines. For example, a precision determination of the polarized PDFs will first come from the EIC.

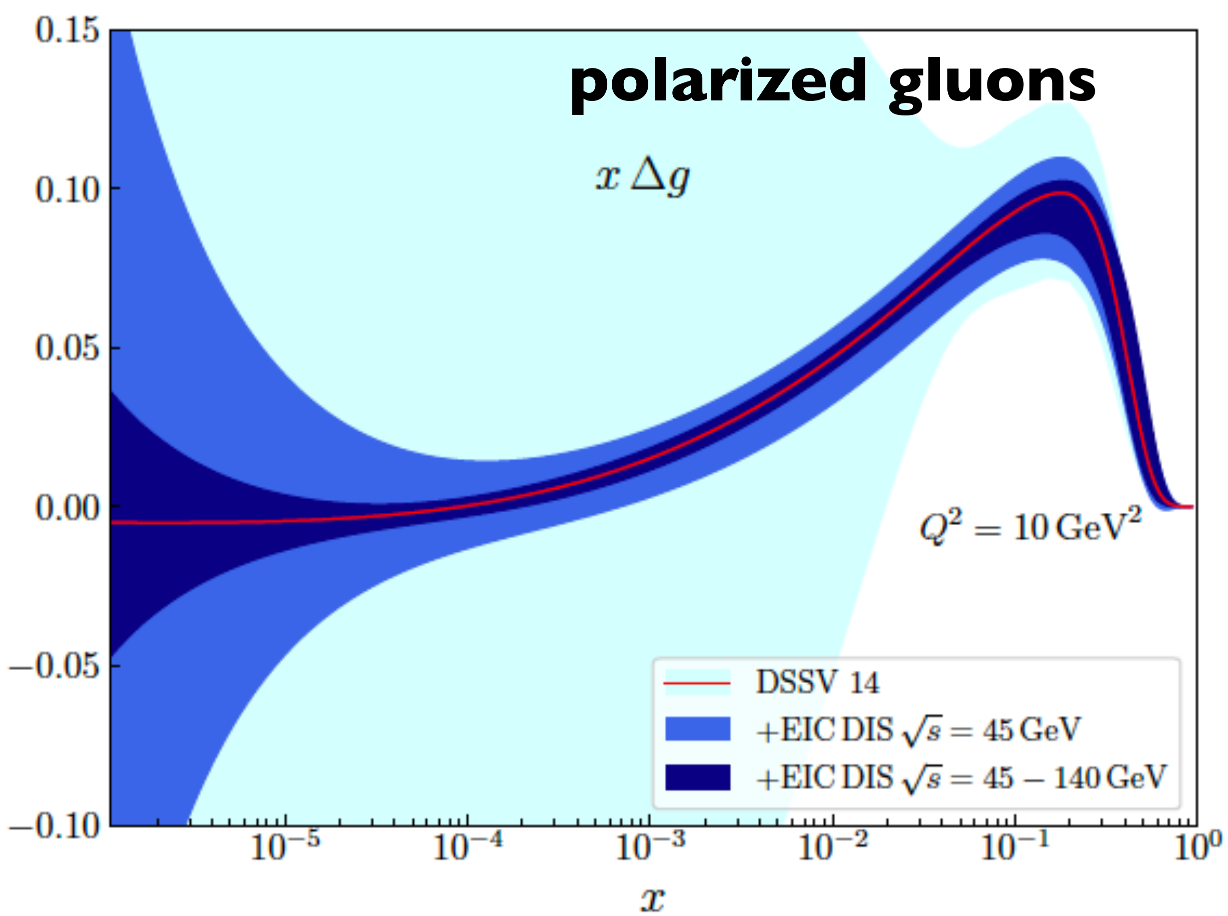

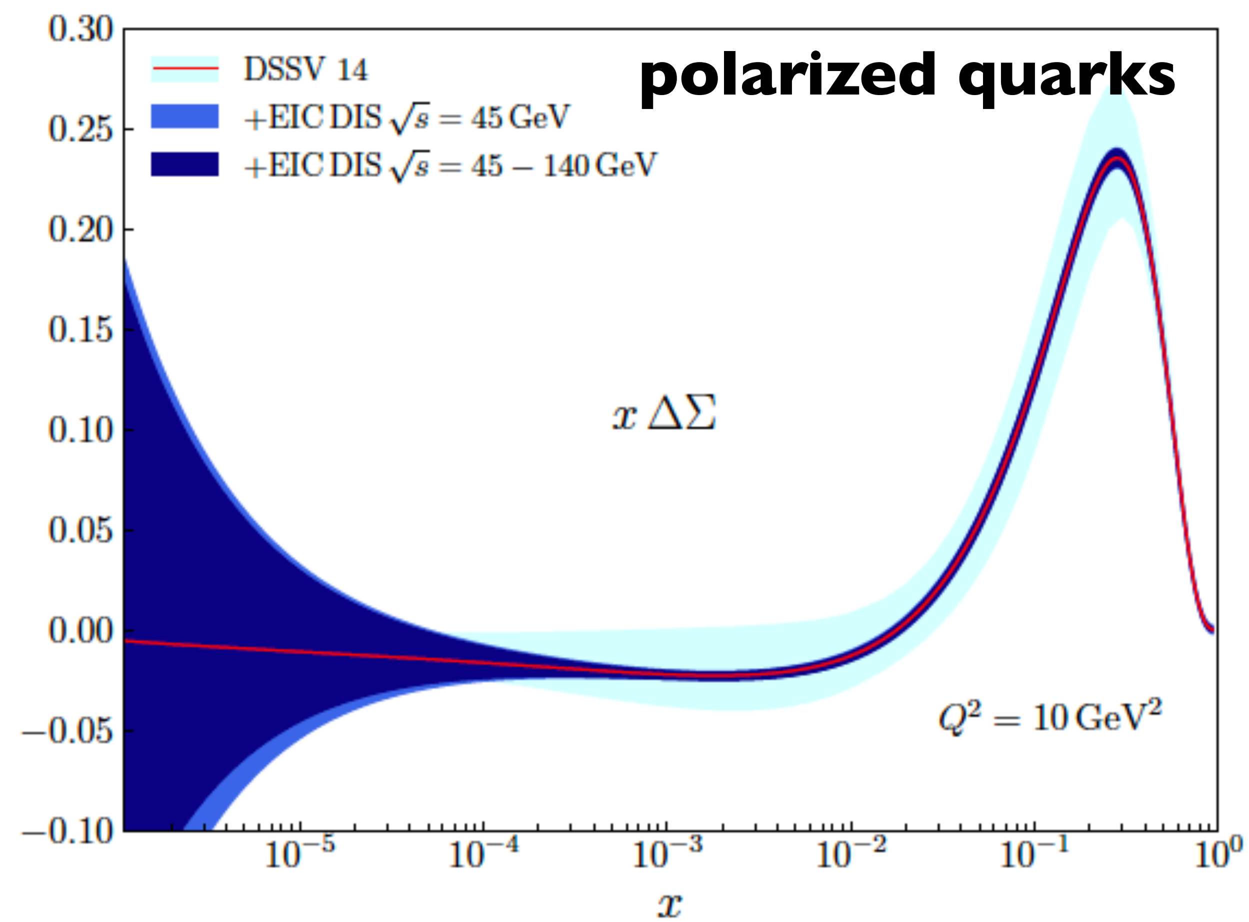

Combination of DIS and pion, kaon SIDIS simulated data. Δg probed through scaling violations of g_1 at much lower x-values than at RHIC

Bora, Lucero, Sassot, Aschenauer, Nunes 2007.08300

Precision jets at the EIC

- The EIC precision is not just for inclusive DIS, but for jets as well. PDF errors are larger than estimated experimental errors for jet production processes. These distributions can improve PDF extractions. They have different systematic errors than g_1 and can provide cross-checks.

Dijet

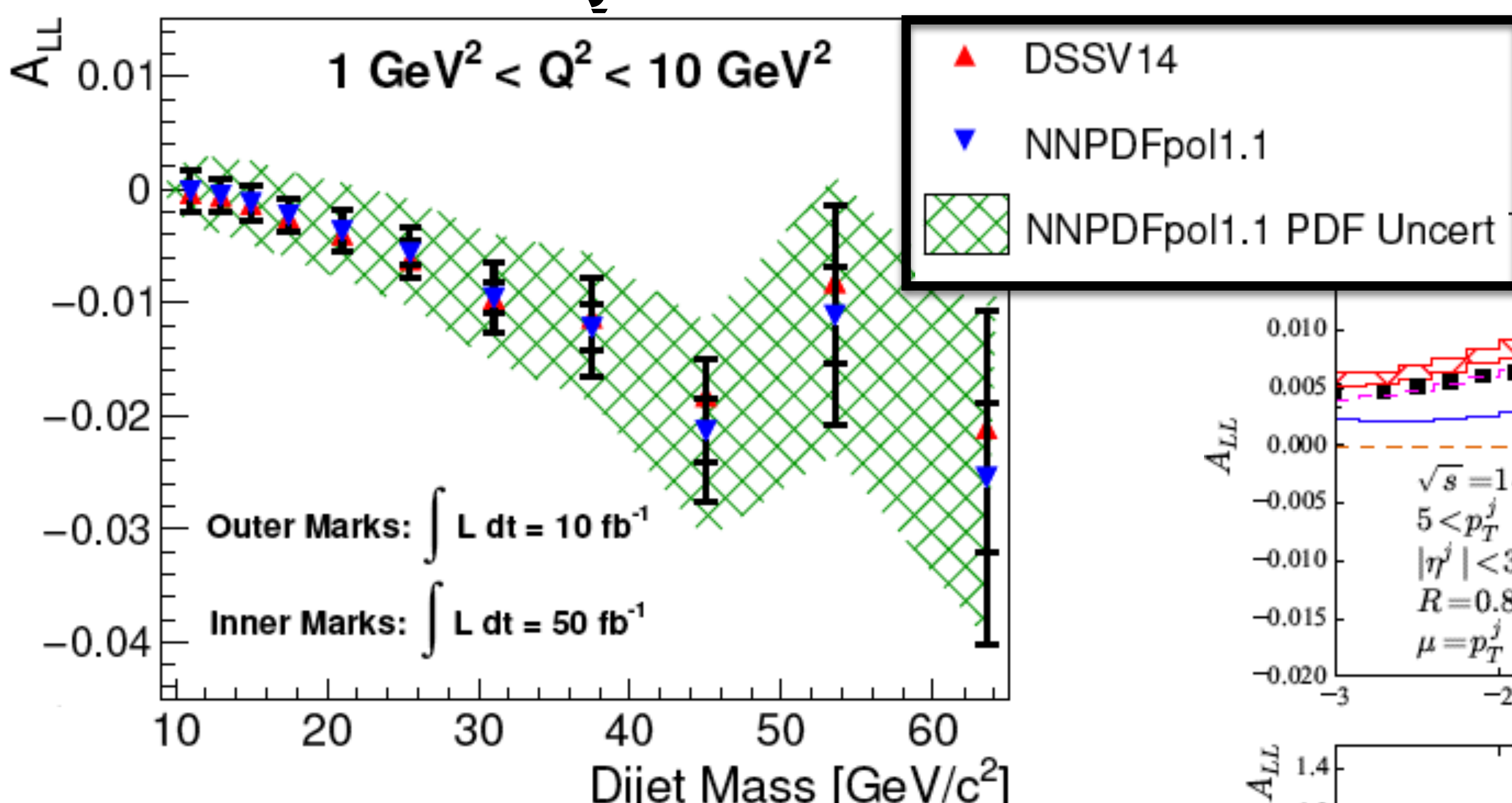

Page, Chu, Aschenauer, 1911.00657

Boughezal, FP, Xing 1806.07311

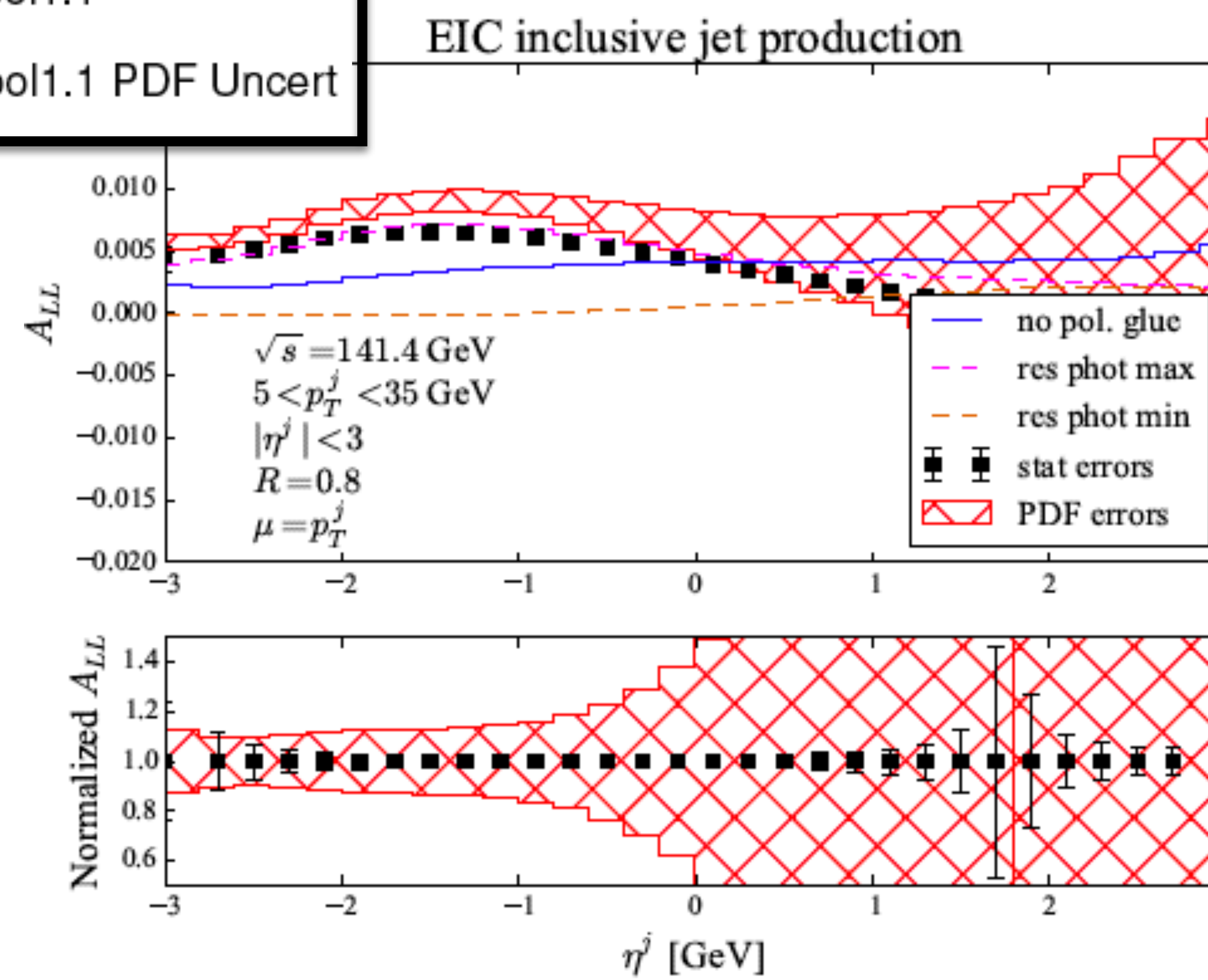

pQCD framework

- The observables relevant for longitudinal structure can be systematically calculated using the perturbative expansion in collinear factorization.

$$\boxed{\sigma_{ep\to X} = \int dx_1 dx_2 f_{i/e}(x_1,\mu^2) f_{j/p}(x_2,\mu^2)\hat{\sigma}_{ij\to X}(x_1,x_2,\mu^2)}$$

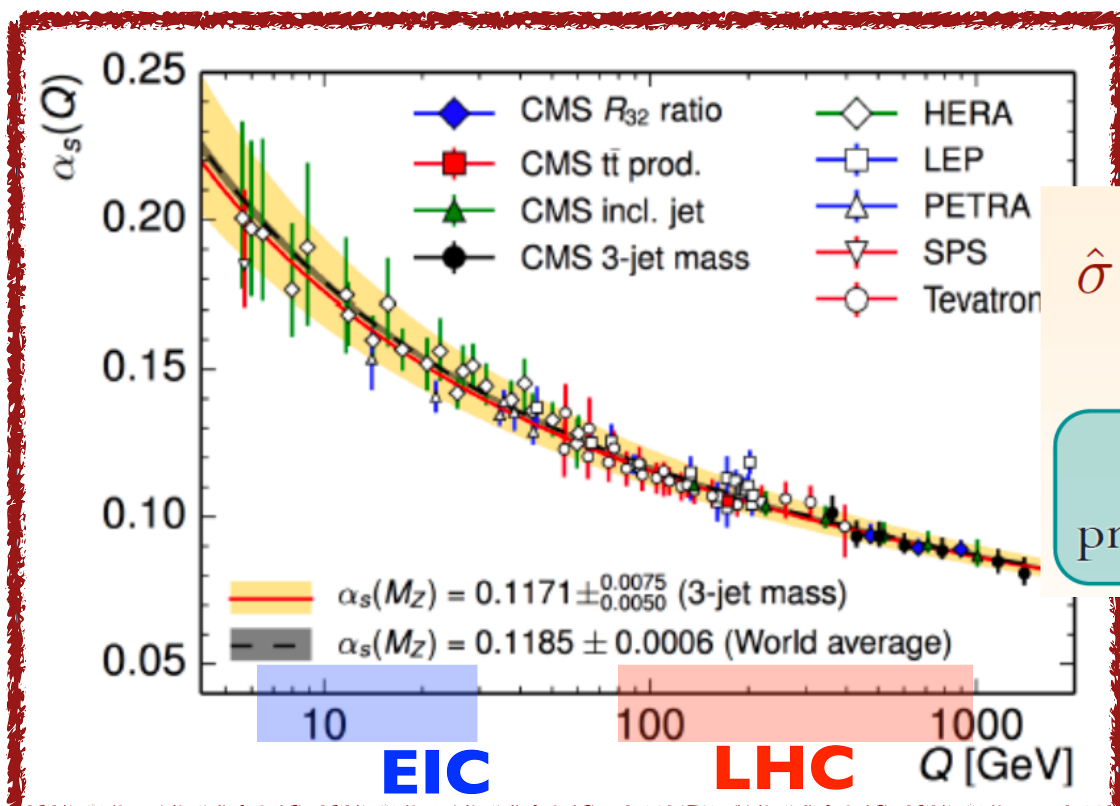

$$\hat{\sigma} = \sigma^{\text{Born}}\left(1 + \frac{\alpha_s}{2\pi}\sigma^{(1)} + \left(\frac{\alpha_s}{2\pi}\right)^2\sigma^{(2)} + \left(\frac{\alpha_s}{2\pi}\right)^3\sigma^{(3)} + \dots\right)$$

LO predictions | NLO corrections | NNLO corrections | NNNLO corrections

EIC: perturbative, but corrections larger than at LHC. Must be included for any quantitative analysis

pQCD to NNLO

- The need for NNLO QCD corrections for precision analyses has been shown to be true for energies ranging from fixed-target to LHC.

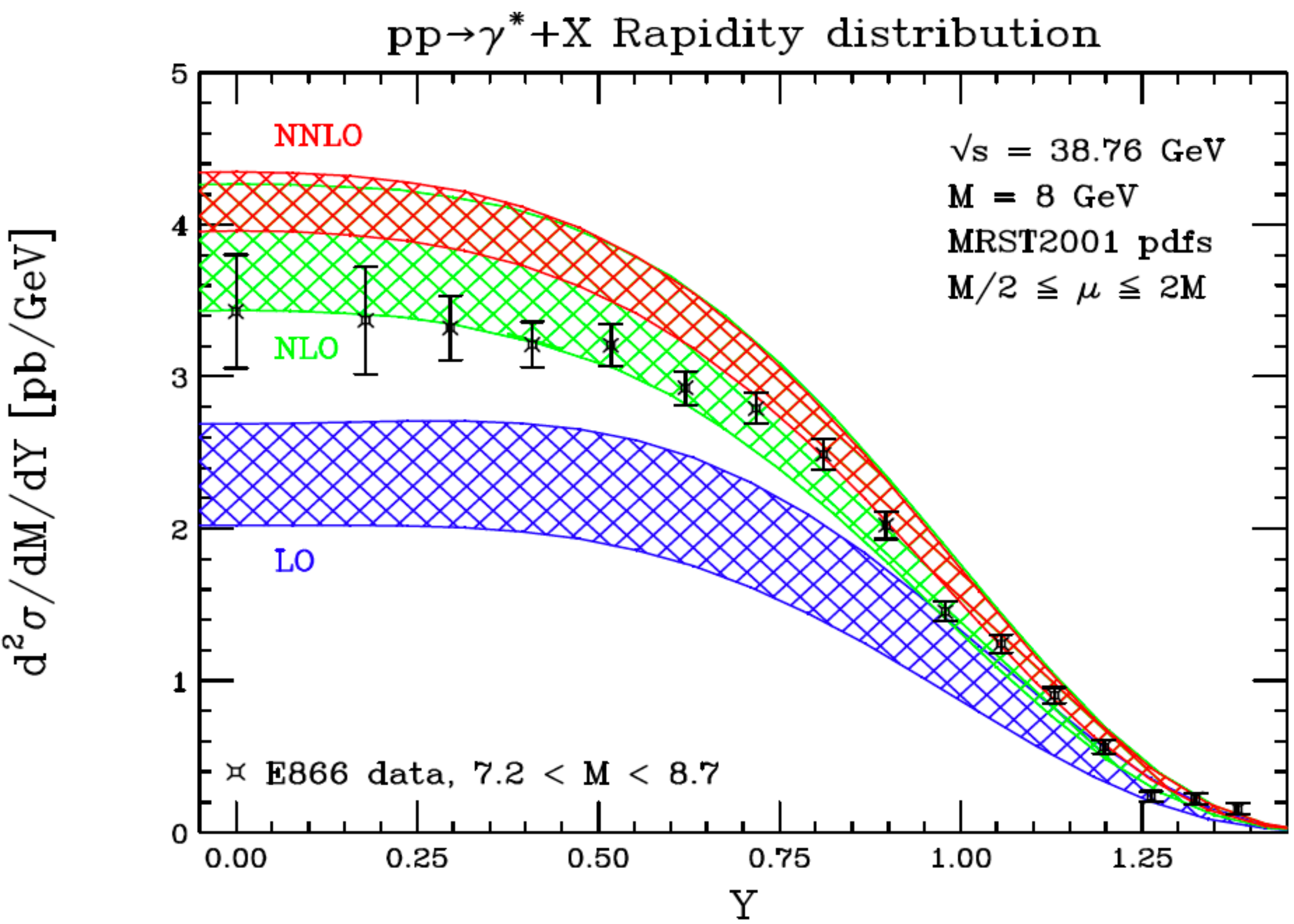

Drell-Yan at fixed-target energies

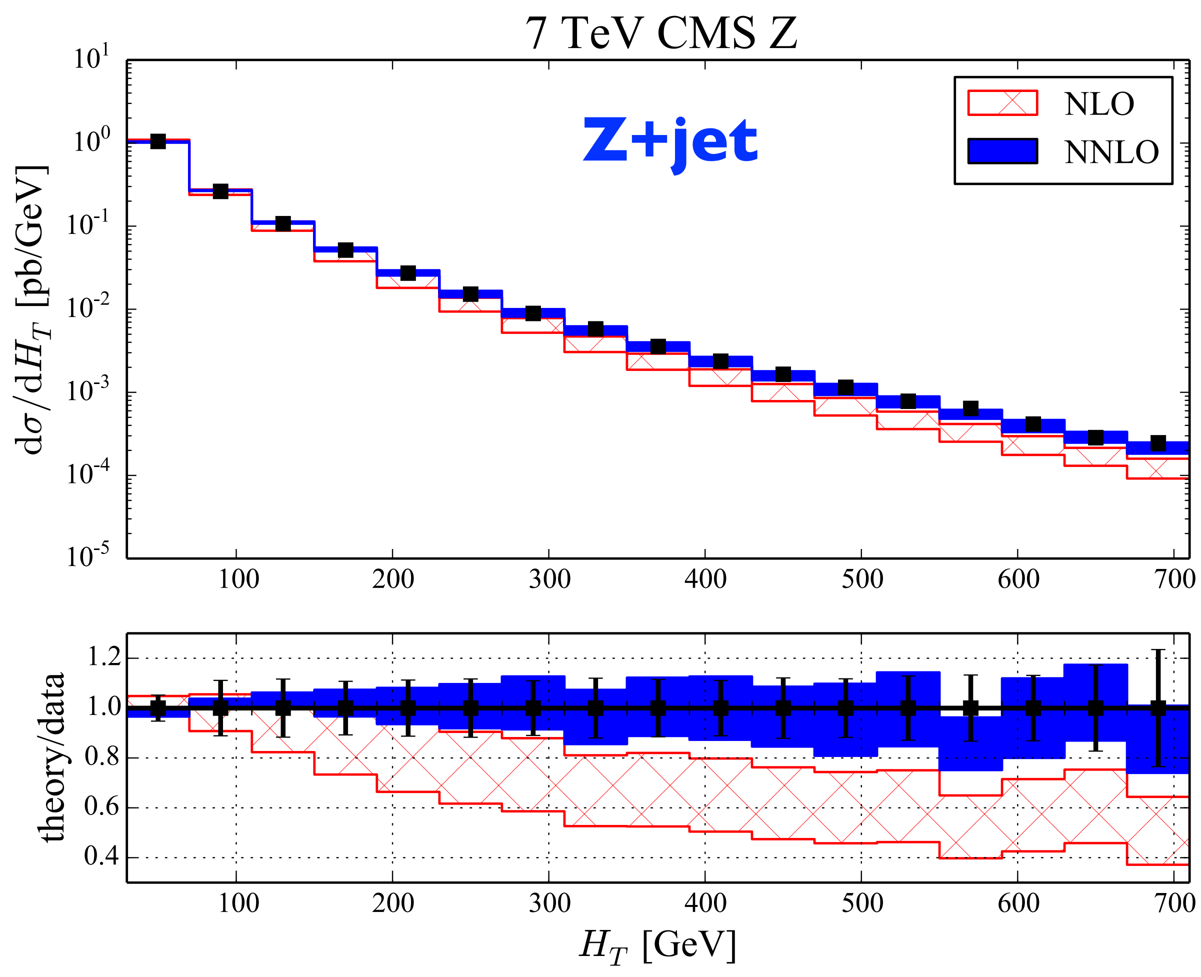

Z+jet background for dark matter searches at the LHC

Anastasiou, Dixon, Menikov, FP
hep-ph/0306192

Boughezal, Liu, FP 1602.05612

The region of pQCD validity

- There are also interesting questions regarding the region of validity of perturbative QCD, which the EIC can help address.

ep→π+X at E_e=48.35 GeV

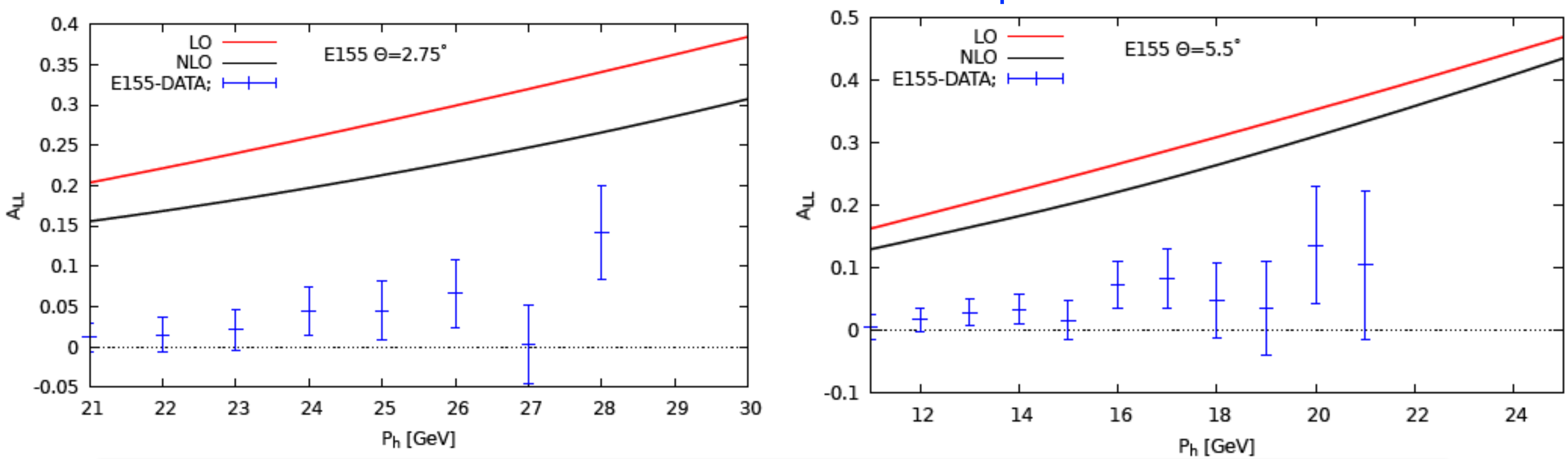

Poor agreement and large corrections for associated asymmetry in hadron production at E155; non-perturbative power corrections? PDFs or FFs? Revisit this issue with jets and the larger kinematic lever arm at the EIC

Hinderer, Schlegel, Vogelsang 1703.10872

Jet and polarized W production to NNLO in QCD

Abelof, Boughezal, Liu, FP 1607.04921

Boughezal, FP, Schubert, Xing 1704.05457

Boughezal, FP, Xing 1806.07311

Boughezal, Li, FP 2101.02214

Framework and setup

- We will first study inclusive jet production and explain how it differs from the usual DIS process. Afterwards we will discuss a motivation for measuring this process at the EIC.

DIS: $eN \to eN$

- lepton tagged
- Cut on Q^2
- hard scale: Q

$q(p_1) + l(p_2) \to q(p_3) + l(p_4)$

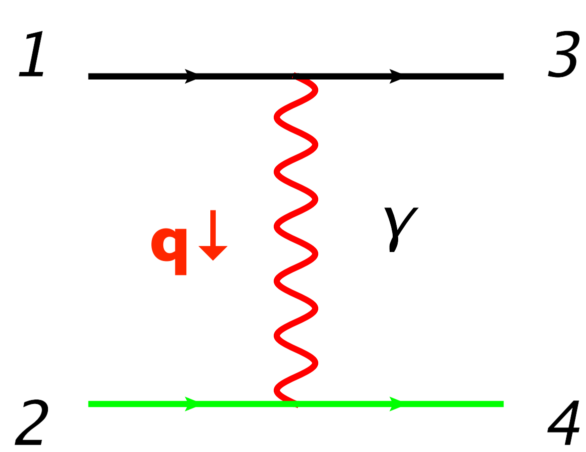

Inclusive jet production: $eN \to jX$

- lepton *not* tagged
- Cut on p_{Tjet}
- hard scale: p_{Tjet}

- Leading order: identical for both processes, lepton recoils against a jet

Inclusive jet production at the EIC

- Three distinct contributions contribute to this process through $O(\alpha_s^2)$ in QCD perturbation theory:

(1) DIS process:
$q_1+e_2 \to q_3+l_4+X$

Begins at $O(\alpha_s^0)$

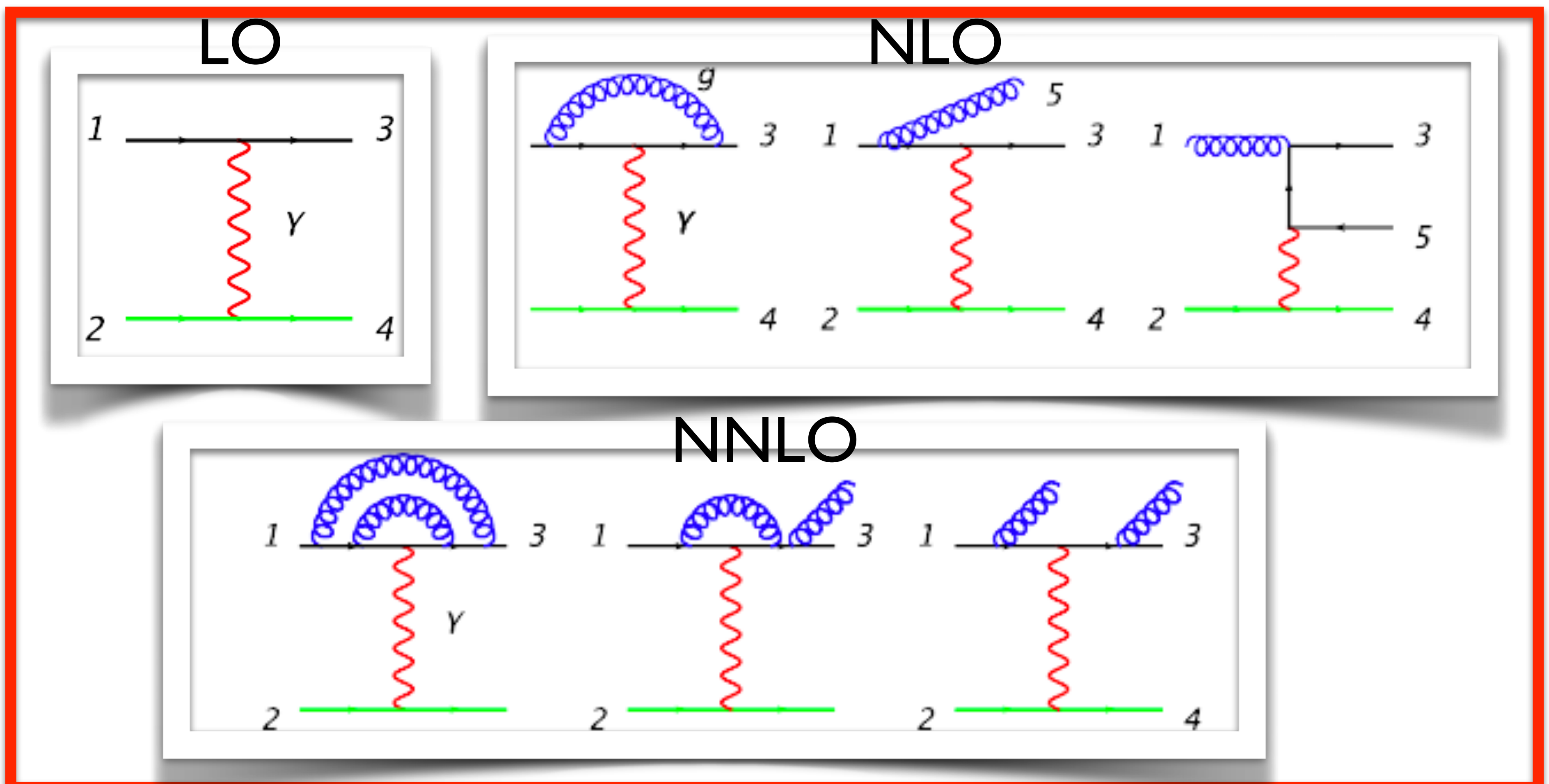

Inclusive jet production at the EIC

(2) Weizsacker-Williams (WW) photon process: $q/g_1+\gamma_2 \rightarrow q_3+g/q_4+X$

When $Q^2 \approx 0$ the final-state electron is collinear to the initial beam, and we can describe this process in terms of a photon PDF up to terms suppressed by the electron mass over the hard scale.

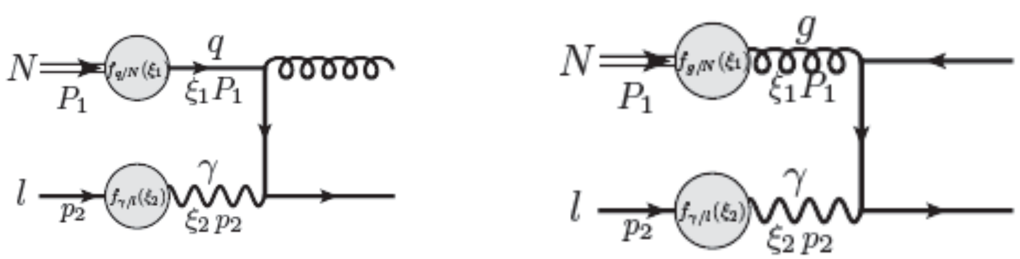

$$f_{\gamma/l}(\xi) = \frac{\alpha}{2\pi} P_{\gamma l}(\xi)\left[\ln\left(\frac{\mu^2}{\xi^2 m_l^2}\right) - 1\right] + \mathcal{O}(\alpha^2)$$

Begins at $O(\alpha_s^1)$

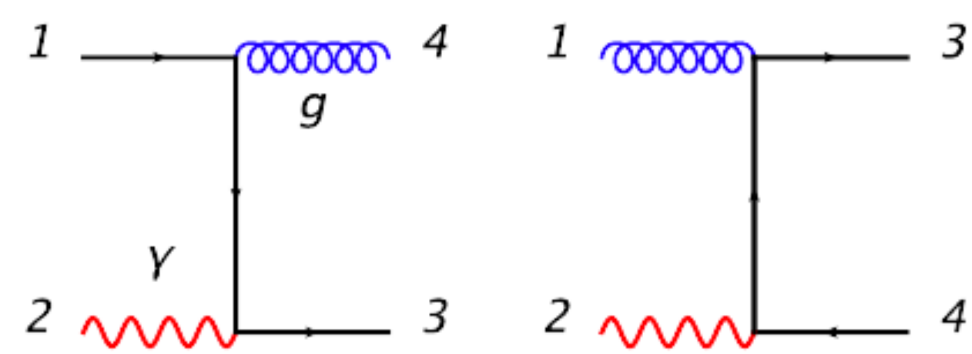

Inclusive jet production at the EIC

(3) Resolved photon process: $q/g_1 + q/g_2 \to q/g_3 + g/q_4 + X$

Again occurs for $Q^2 \approx 0$. This time the photon splits to partons at low virtualities and leads to a non-perturbative contribution.

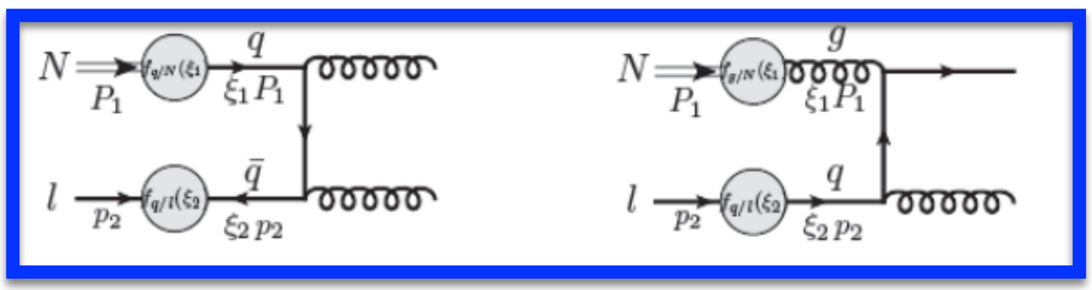

Formally begins at $O(\alpha_s^2)$

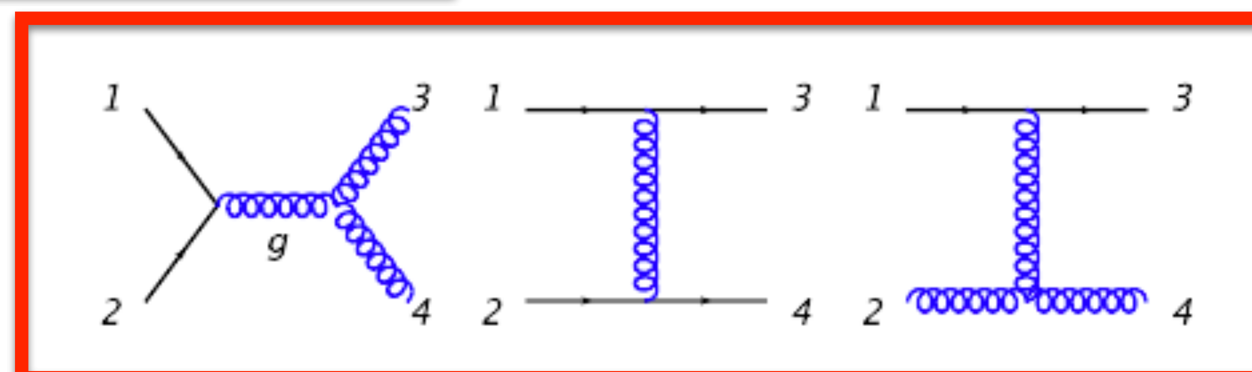

$$\int \frac{d\xi_1 d\xi_2 dy}{\xi_1 \xi_2 y} f_{i/P}(\xi_1) f_{j/\gamma}(\xi_2/y) P_{\gamma l}(y) \hat{\sigma}_{ij}(y)$$

proton PDFs

photon PDFs

QED splitting function

Jets and longitudinal photon structure

- Polarized jet production at the EIC will provide our first view of the longitudinal structure of polarized photons, which is currently based on models only.

Chu, Aschenauer, Lee, Zheng 1705.08831

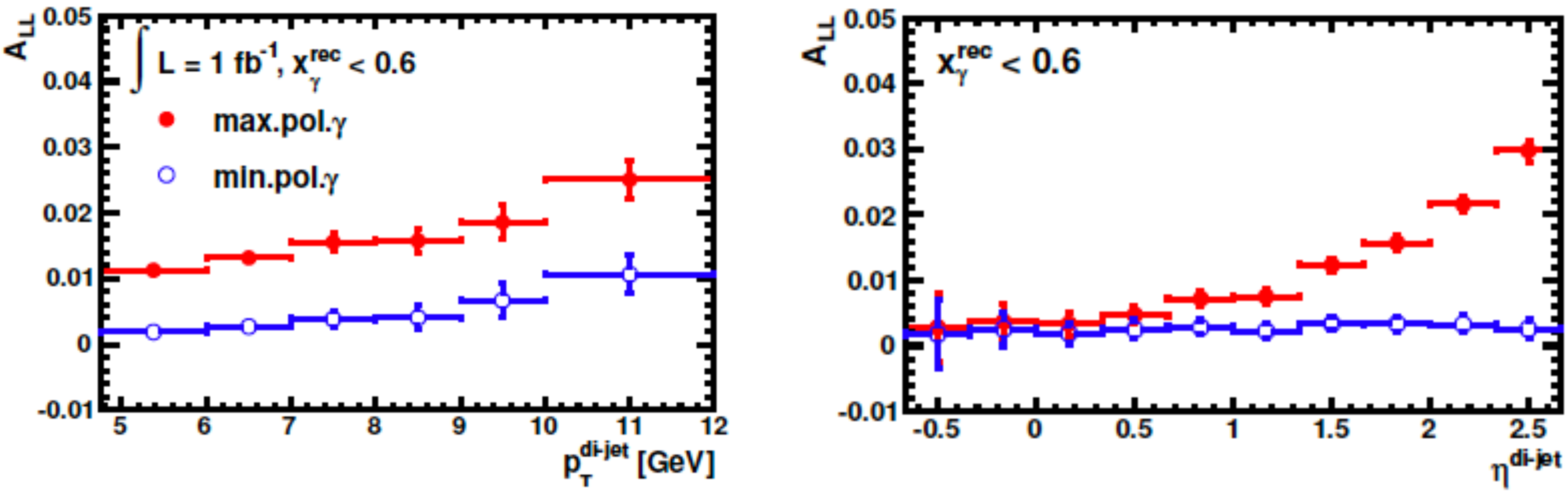

minimal: $\Delta f^\gamma(x,\mu^2) = 0$

maximal: $\Delta f^\gamma(x,\mu^2) = f^\gamma(x,\mu^2)$

Calculations to NNLO in QCD

- Most difficult piece is the combination of double-virtual, real-virtual and double-real contributions to cancel IR singularities. Significant progress in solving this problem for LHC applications.

$$\boxed{\tau_N = \sum_k \min\{n_i \cdot q_k\}}$$

N-jettiness, an event shape variable (similar to thrust)

light-like directions of initial beams and final-state jets

momenta of final-state partons

Stewart, Tackmann, Waalewijn 1004.2489

Intuition: **$\tau_N \sim 0$**: all radiation is either soft, or collinear to a beam/jet

$\tau_N > 0$: at least one additional jet beyond Born level is resolved

N-jettiness subtraction

Boughezal, Focke, Liu, FP 1504.02131; Gaunt, Stahlhofen, Tackmann 1505.04794

$$\boxed{\sigma = \int d\tau_N \frac{d\sigma}{d\tau_N}\theta(\tau^{cut} - \tau_N) + \int d\tau_N \frac{d\sigma}{d\tau_N}\theta(\tau_N - \tau^{cut})}$$

a simpler effective theory description is available for the region

have one more resolved jet than at Born level; **only need NLO in this region!**

$$\boxed{\frac{d\sigma}{d\tau_N}(\tau_N \ll Q) \sim H \otimes B_a \otimes S \otimes \left[\prod_{n=1}^{N} J_n\right]}$$

hard scales in the process (e.g., transverse momenta of jets)

describes hard radiation

describes radiation collinear to initial-state beams (matches onto collinear PDFs); ***universal***

describes soft radiation; ***universal***

describes radiation collinear to final-state jets; ***universal***

Inclusive jet production: unpolarized

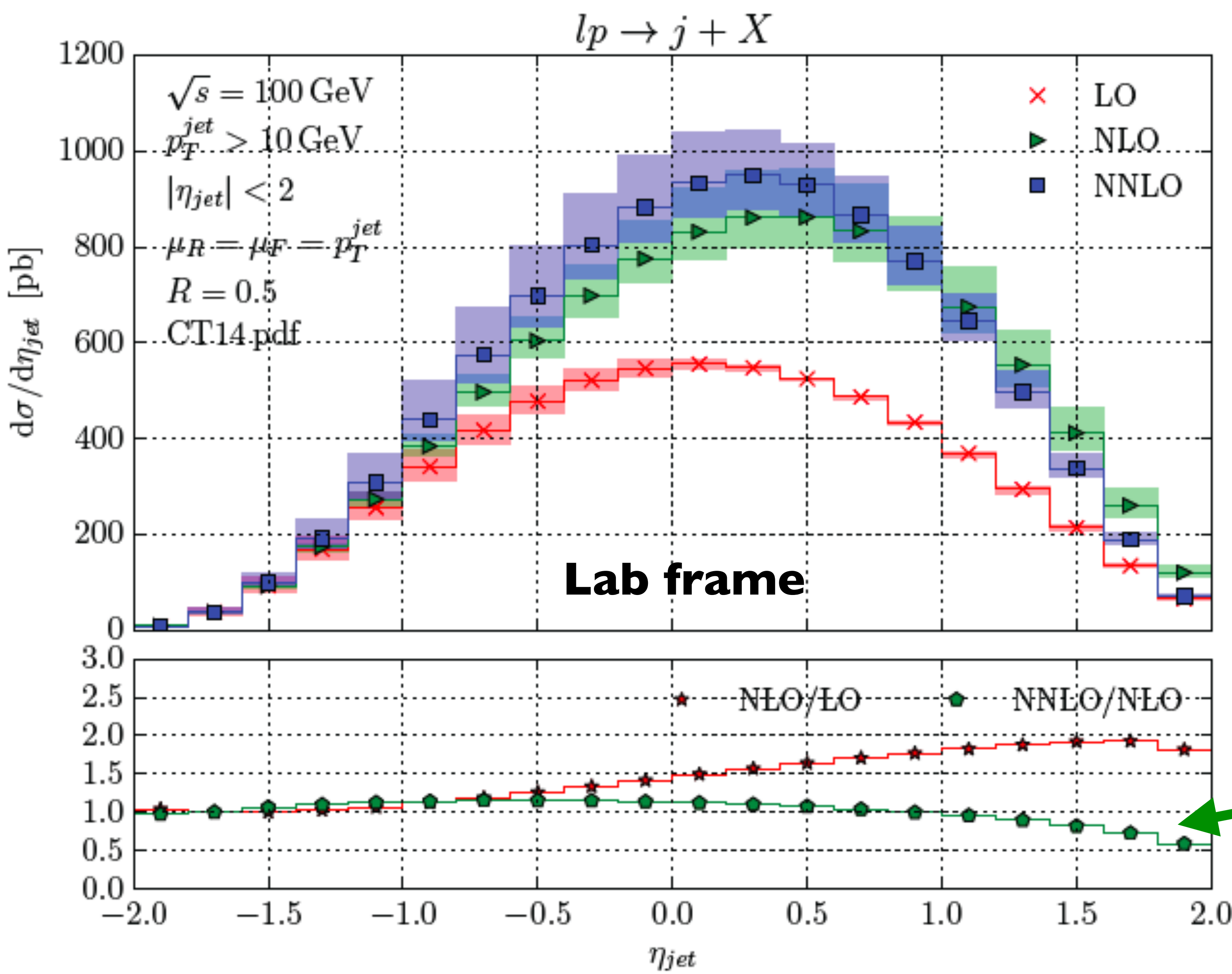

- Requires $O(\alpha_s^2)$ for accurate prediction; WW photons at $O(\alpha_s)$ give large correction (Hinderer, Schlegel, Vogelsang 1505.06415)
- Larger-than-expected scale dependence at $O(\alpha_s^2)$ from resolved photon terms
- $O(\alpha_s^2)$ leads to slight decrease at high eta

Abelof, Boughezal, X. Liu, FP 1607.04921

Split into partonic components

- Jet distributions at the EIC are an excellent probe of PDFs; no single channel dominates over all of phase space, indicating that different kinematic regions provide access to different partonic luminosities.

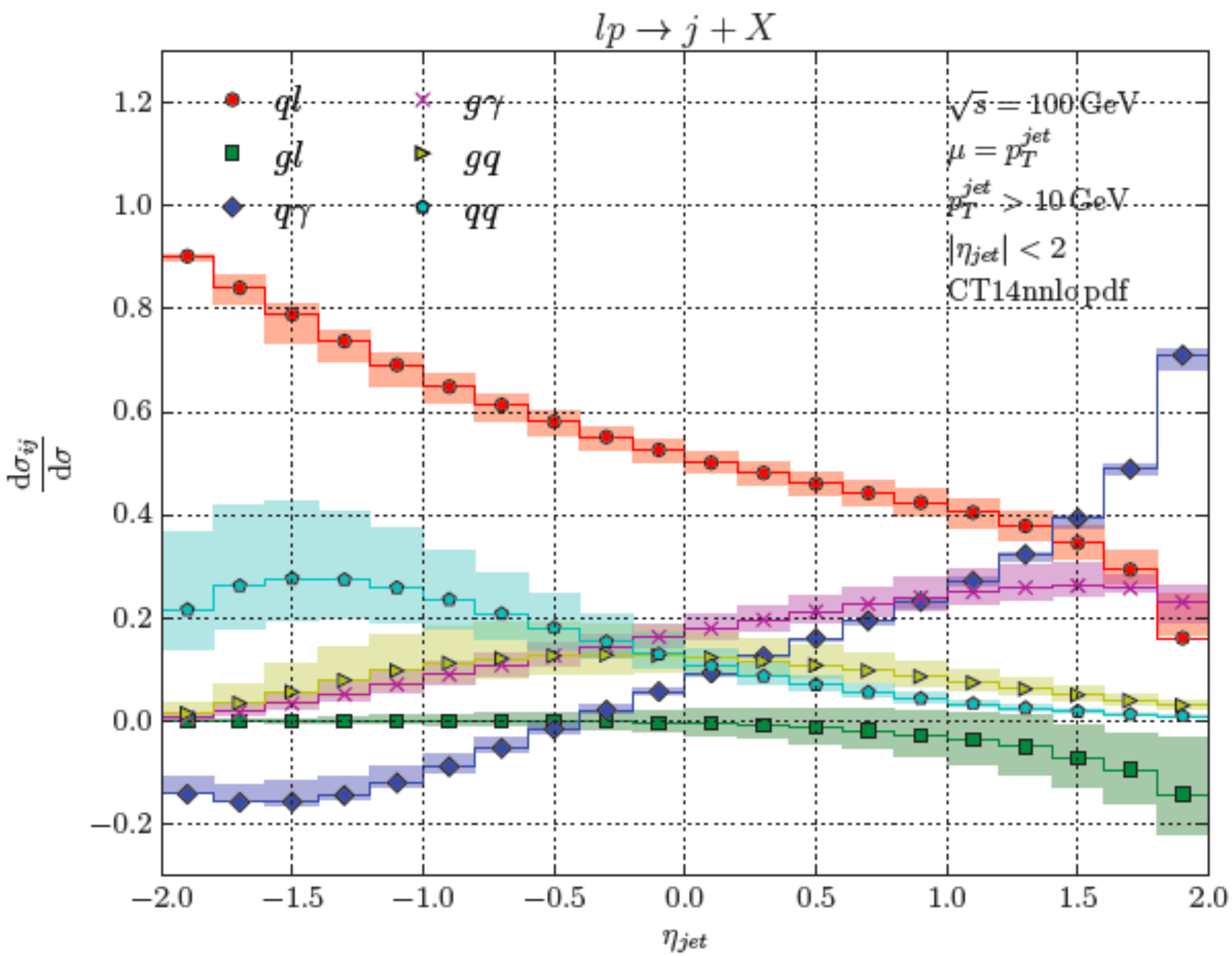

Abelof, Boughezal, X. Liu, FP 1607.04921

Polarized collisions

- We are interested in polarized proton structure at an EIC; need to extend N-jettiness subtraction to handle polarized collisions
- Schematic form of factorization theorem for unpolarized and longitudinally polarized collisions:

unpolarized: $d\sigma/d\tau \sim H \otimes B \otimes J \otimes S$

polarized: $d\Delta\sigma/d\tau \sim \Delta H \otimes \Delta B \otimes J \otimes S$

known helicity-dependent 2-loop virtual corrections

two-loop helicity-dependent beam function

Boughezal, FP, Schubert, Xing 1704.05457

Phenomenology of polarized collisions

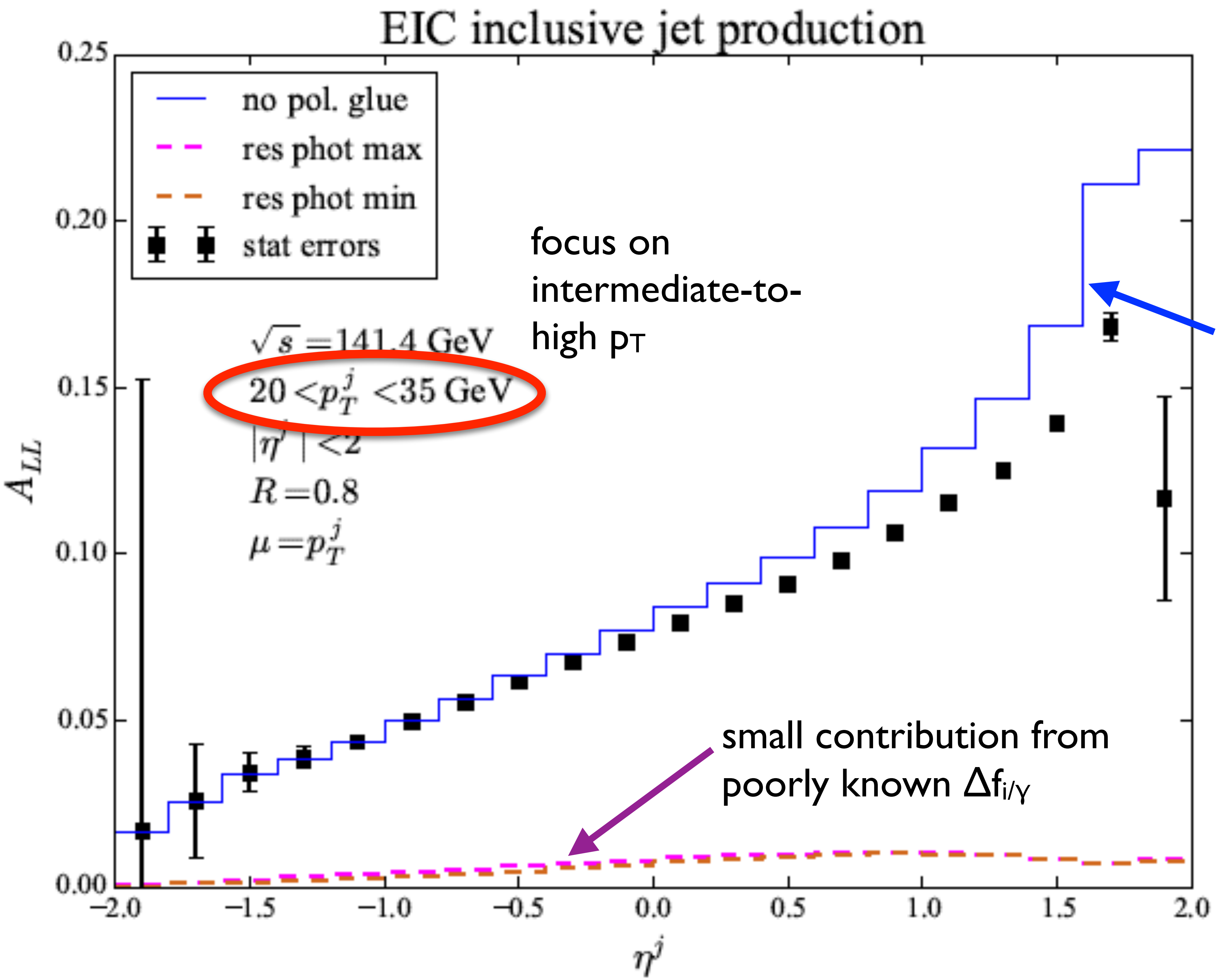

focus on intermediate-to-high p_T

small contribution from poorly known $\Delta f_{i/\gamma}$

NLO analysis with resolved photons

turning off polarized gluon leads to adifferent shape of the jet pseudorapidity distribution; larger than estimated statistical errors

Sensitive to $\Delta fg/P$ through WW photon processes at intermediate jet momenta

Boughezal, FP, Xing PRD98 (2018)

Another application: W at RHIC

- Longitudinal spin asymmetries in W production provide a glimpse of flavor structure in the polarized quark sea

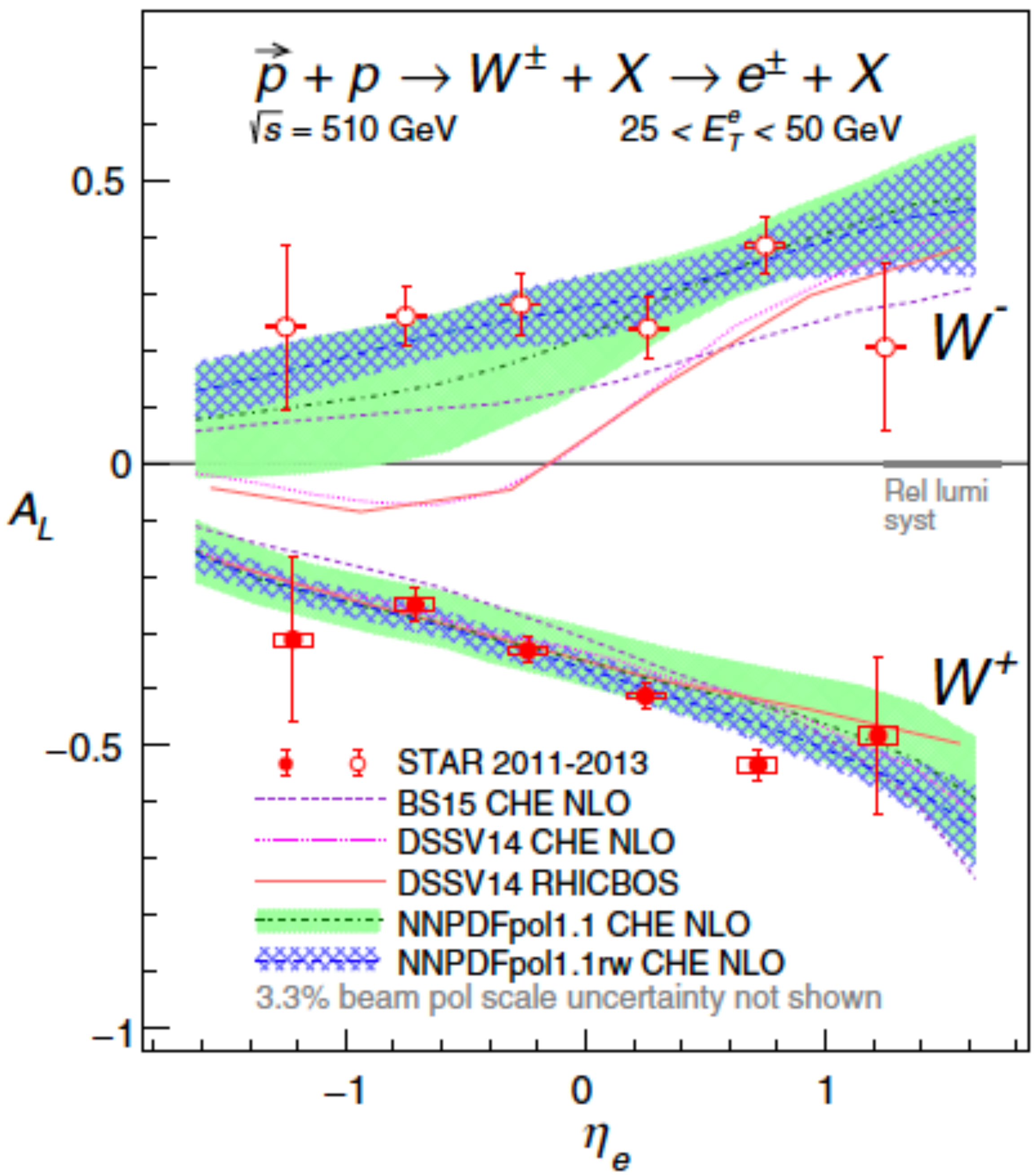

$$A_L \equiv (\sigma_+ - \sigma_-)/(\sigma_+ + \sigma_-)$$

$$A_L^{W^+}(y_W) \propto \frac{\Delta\bar{d}(x_1)u(x_2) - \Delta u(x_1)\bar{d}(x_2)}{\bar{d}(x_1)u(x_2) + u(x_1)\bar{d}(x_2)}$$

$$A_L^{W^-}(y_W) \propto \frac{\Delta\bar{u}(x_1)d(x_2) - \Delta d(x_1)\bar{u}(x_2)}{\bar{u}(x_1)d(x_2) + d(x_1)\bar{u}(x_2)}$$

$$y_W \gg 0 \to x_1 \gg x_2 : A_L^{W^+} \approx -\frac{\Delta u(x_1)}{u(x_1)}, A_L^{W^-} \approx -\frac{\Delta d(x_1)}{d(x_1)}$$

$$y_W \ll 0 \to x_2 \gg x_1 : A_L^{W^+} \approx \frac{\Delta\bar{d}(x_1)}{\bar{d}(x_1)}, A_L^{W^-} \approx \frac{\Delta\bar{u}(x_1)}{\bar{u}(x_1)}$$

$A_L^{W-}>0$ and $A_L^{W-+}<0$ at negative η_e indicate a positive $\Delta\bar{u}$-$\Delta\bar{d}$

W production at RHIC

- Longitudinal spin asymmetries in W production provide a glimpse of flavor structure in the polarized quark sea

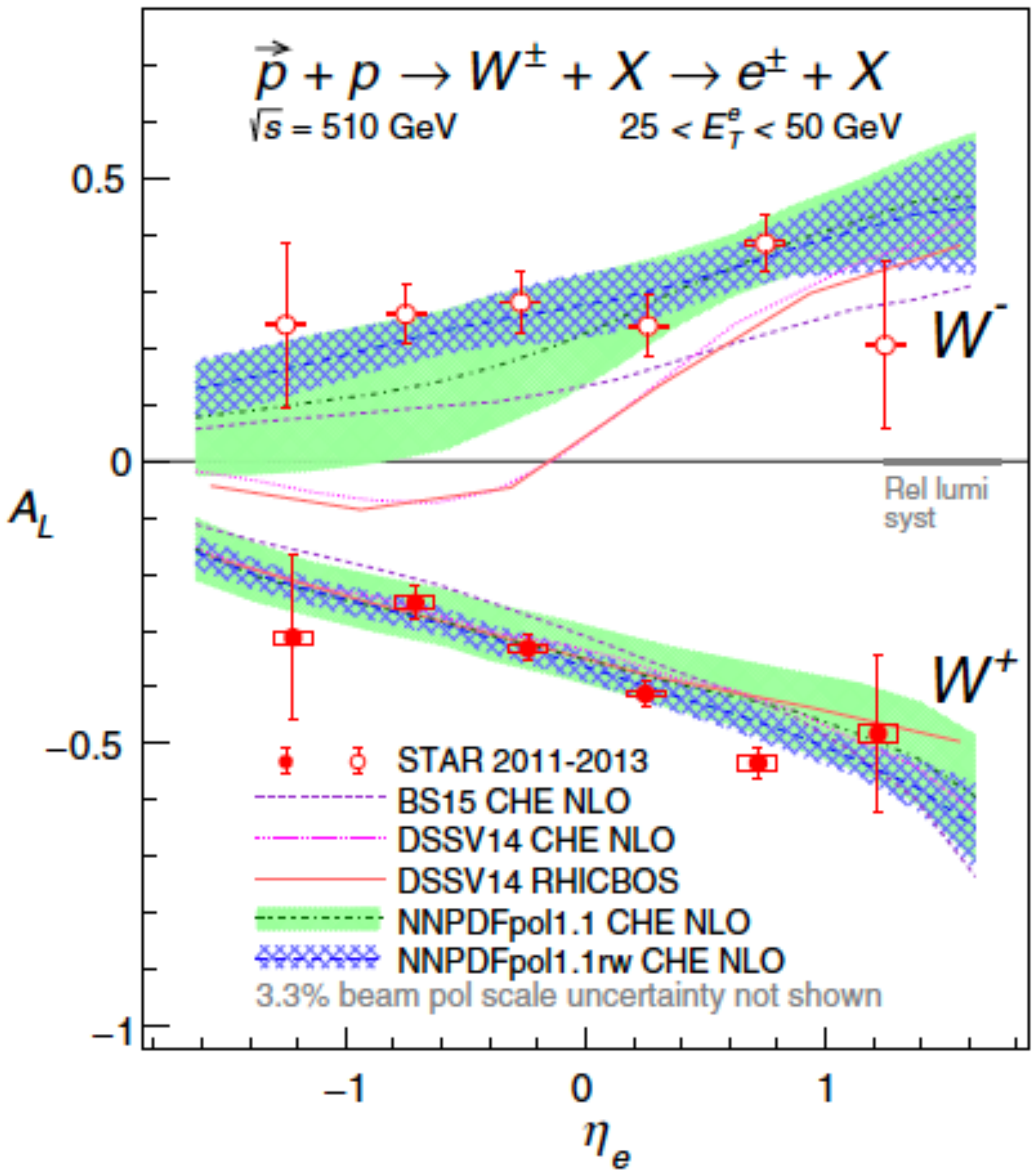

$$A_L \equiv (\sigma_+ - \sigma_-)/(\sigma_+ + \sigma_-)$$

$$A_L^{W^+}(y_W) \propto \frac{\Delta\bar{d}(x_1)u(x_2) - \Delta u(x_1)\bar{d}(x_2)}{\bar{d}(x_1)u(x_2) + u(x_1)\bar{d}(x_2)}$$

$$A_L^{W^-}(y_W) \propto \frac{\Delta\bar{u}(x_1)d(x_2) - \Delta d(x_1)\bar{u}(x_2)}{\bar{u}(x_1)d(x_2) + d(x_1)\bar{u}(x_2)}$$

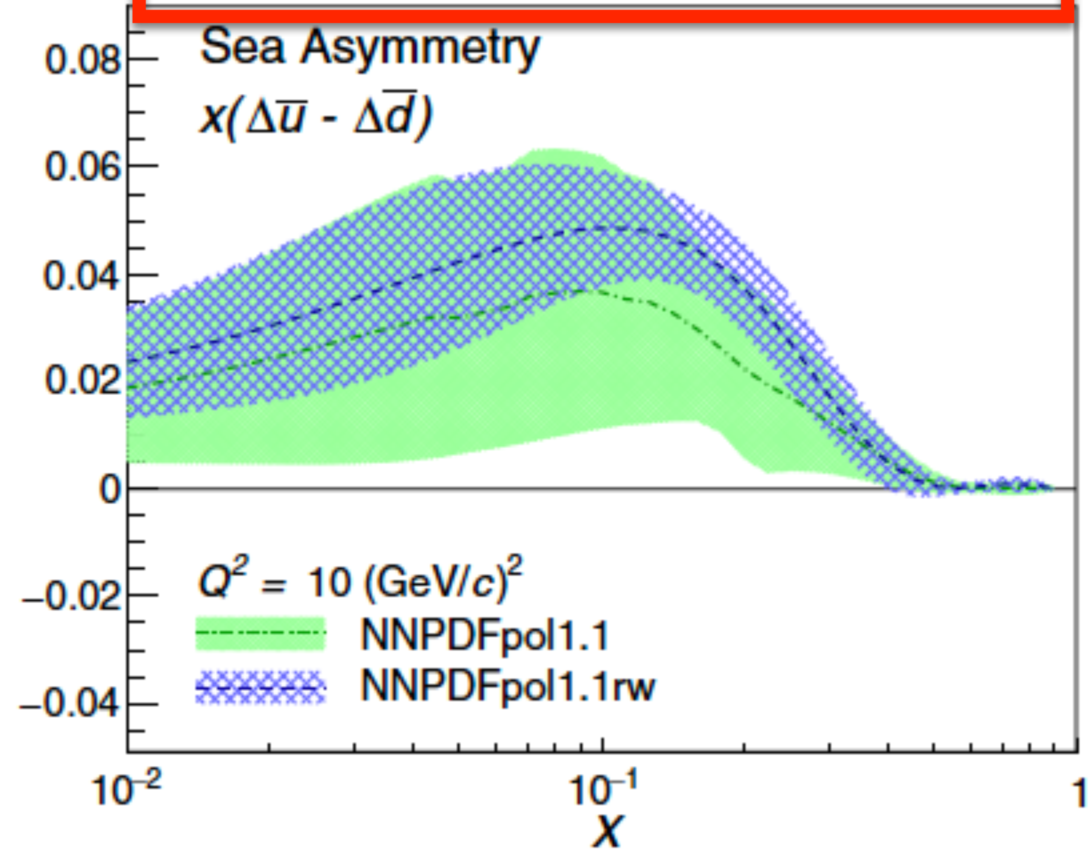

W production at RHIC

- First use of the NNLO polarized beam functions. All distributions show excellent stability under perturbative QCD corrections. An important step toward a global fit of polarized data to NNLO.

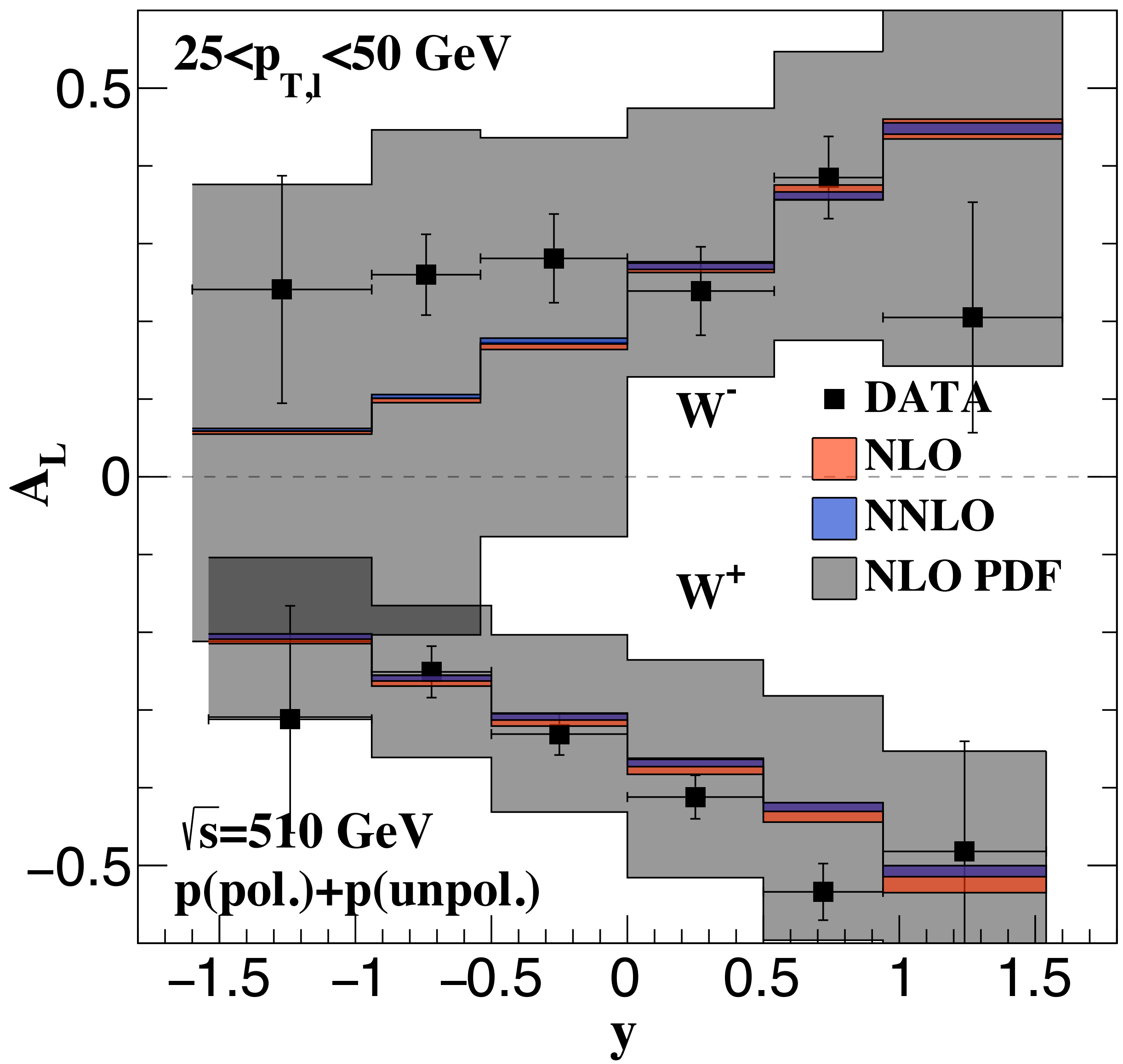

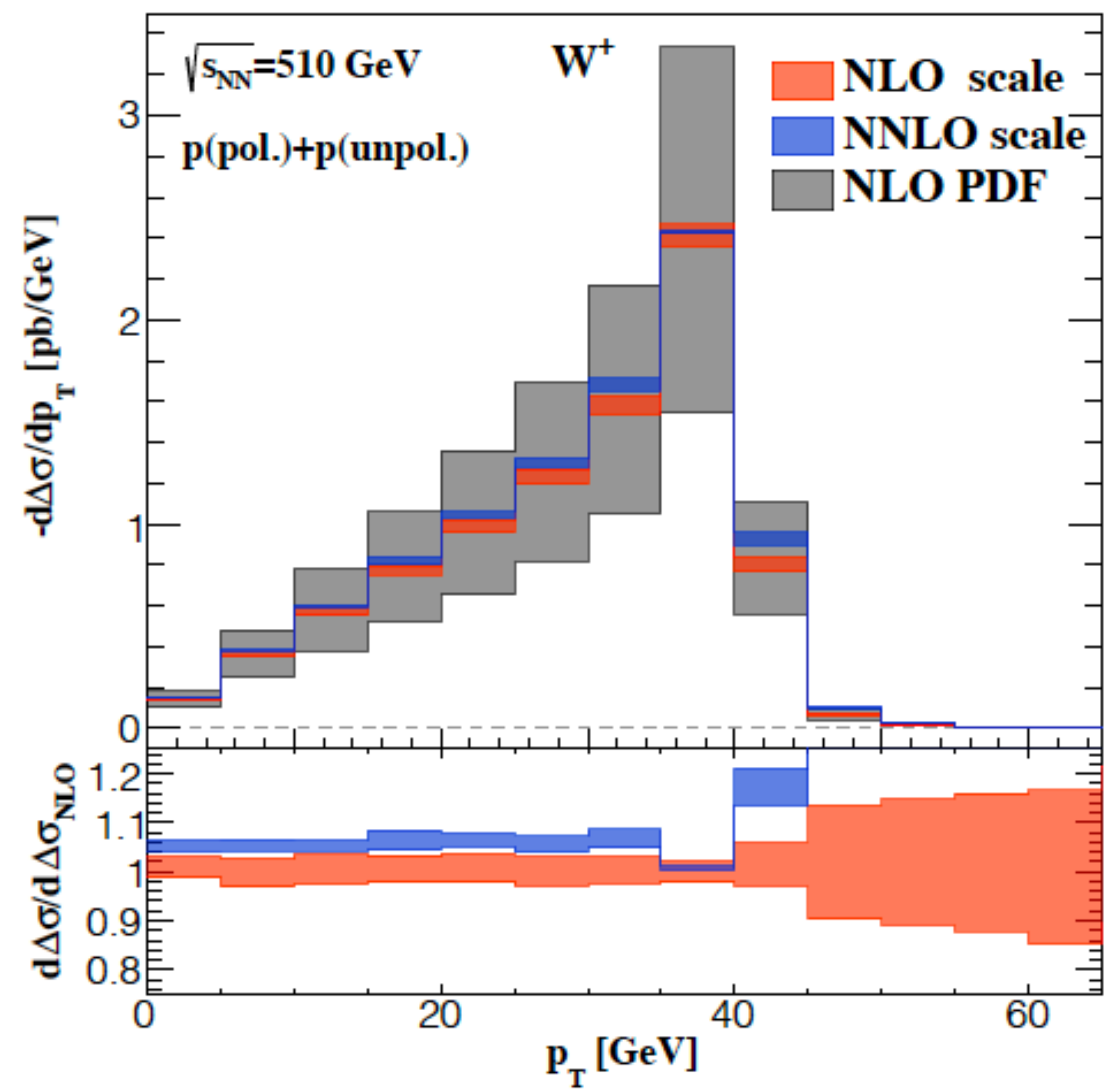

Boughezal, H.T. Li, FP 2101.02214

Synergy between LHC and EIC searches for BSM physics

Boughezal, FP, Wiegand 2004.00748

Boughezal, Emmert, Kutz, Mantry, Nycz, FP, Şimşek, Wiegand, Zheng 2204.07557

BSM searches at the LHC

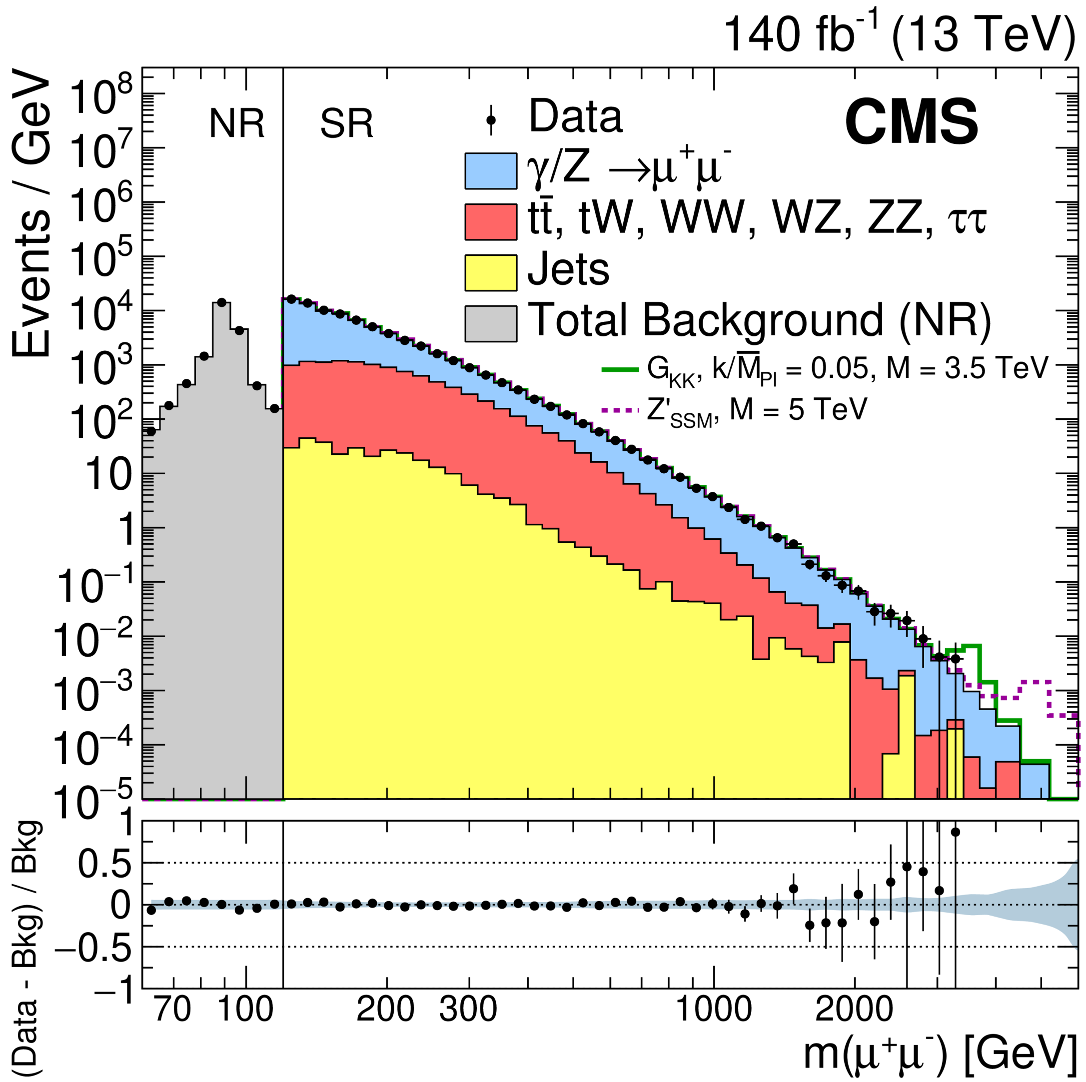

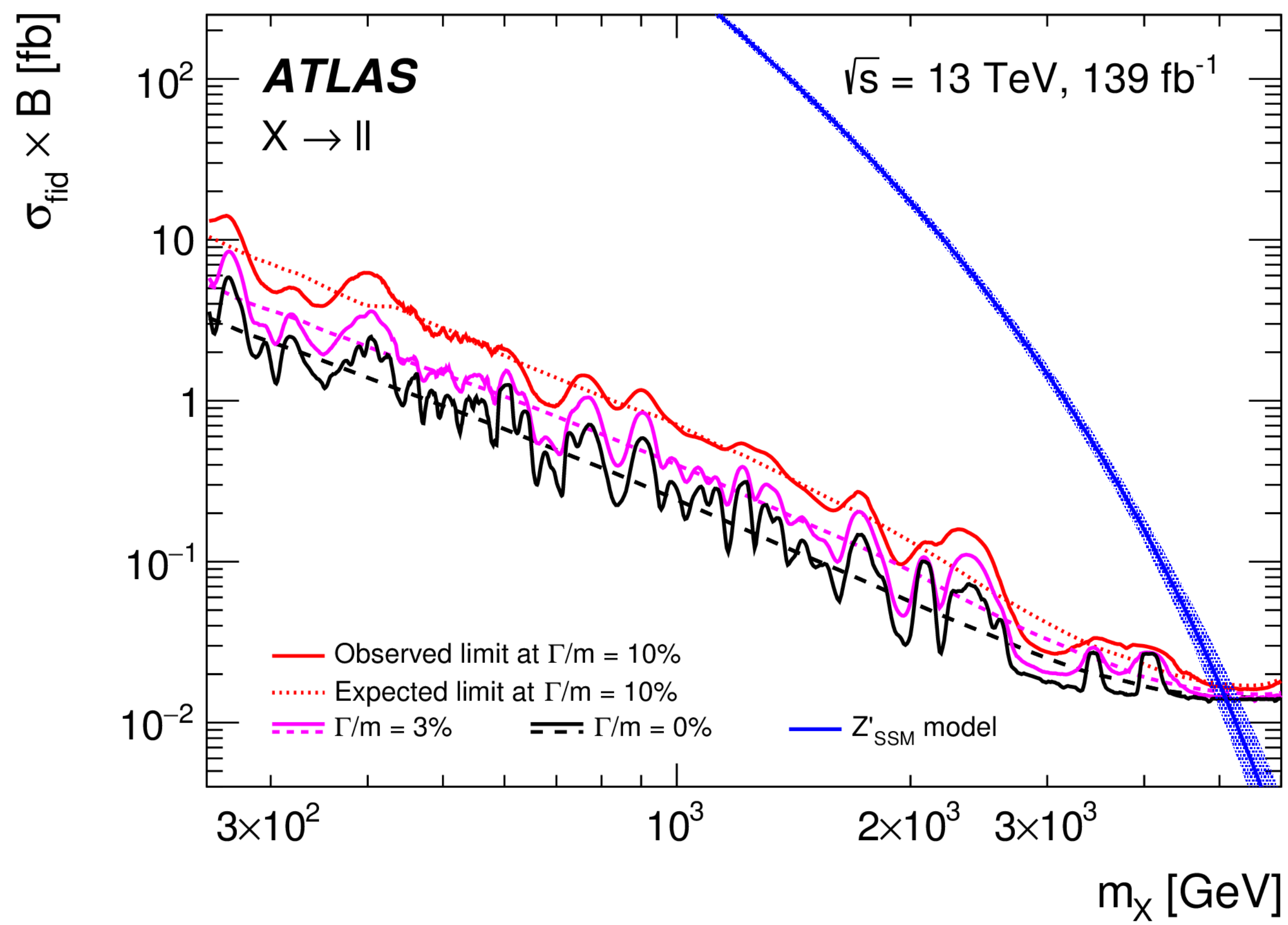

Sensitivity to new resonances in the Drell-Yan channel has reached 5 TeV in some models. Suggests a mass gap between SM and new physics; indirect searches increasingly important

Framework for future searches

- Two approaches for future indirect searches:
  - Formulate specific BSM models, calculate predictions for the LHC and other experiments
  - Adopt an EFT framework that encapsulates a broad swath of possible BSM theories

- Standard Model Effective Field Theory (SMEFT): all operators consistent with SM symmetries, containing SM particles, and assuming a mass gap to any new physics

$$\boxed{\mathcal{L} = \mathcal{L}_{SM} + \frac{1}{\Lambda^2}\sum_i C_{6,i}\mathcal{O}_{6,i} + \frac{1}{\Lambda^4}\sum_i C_{8,i}\mathcal{O}_{8,i}}$$

Dimension-6 **Dimension-8**

$\Lambda \gg M_{SM}$, E

Expand in large Λ

Warsaw basis

- Complete and independent dim-6 basis known: 2499 baryon conserving operators for 3 fermion generations; (can reduce assuming MFV, etc. to O(100))

Grzadkoswki, Iskrzynski, Misiak, Rosiek 1008.4884; Brivio, Jiang, Trott 1709.06492

X^3		φ^6 and $\varphi^4 D^2$		$\psi^2\varphi^3$	
Q_G	$f^{ABC}G_\mu^{A\nu}G_\nu^{B\rho}G_\rho^{C\mu}$	Q_φ	$(\varphi^\dagger\varphi)^3$	$Q_{e\varphi}$	$(\varphi^\dagger\varphi)(\bar l_p e_r \varphi)$
$Q_{\widetilde G}$	$f^{ABC}\widetilde G_\mu^{A\nu}G_\nu^{B\rho}G_\rho^{C\mu}$	$Q_{\varphi\Box}$	$(\varphi^\dagger\varphi)\Box(\varphi^\dagger\varphi)$	$Q_{u\varphi}$	$(\varphi^\dagger\varphi)(\bar q_p u_r \widetilde\varphi)$
Q_W	$\varepsilon^{IJK}W_\mu^{I\nu}W_\nu^{J\rho}W_\rho^{K\mu}$	$Q_{\varphi D}$	$\left(\varphi^\dagger D^\mu\varphi\right)^\star\left(\varphi^\dagger D_\mu\varphi\right)$	$Q_{d\varphi}$	$(\varphi^\dagger\varphi)(\bar q_p d_r \varphi)$
$Q_{\widetilde W}$	$\varepsilon^{IJK}\widetilde W_\mu^{I\nu}W_\nu^{J\rho}W_\rho^{K\mu}$				

$X^2\varphi^2$		$\psi^2 X\varphi$		$\psi^2\varphi^2 D$	
$Q_{\varphi G}$	$\varphi^\dagger\varphi\, G^A_{\mu\nu}G^{A\mu\nu}$	Q_{eW}	$(\bar l_p\sigma^{\mu\nu}e_r)\tau^I\varphi W^I_{\mu\nu}$	$Q_{\varphi l}^{(1)}$	$(\varphi^\dagger i\overleftrightarrow{D}_\mu\varphi)(\bar l_p\gamma^\mu l_r)$
$Q_{\varphi\widetilde G}$	$\varphi^\dagger\varphi\, \widetilde G^A_{\mu\nu}G^{A\mu\nu}$	Q_{eB}	$(\bar l_p\sigma^{\mu\nu}e_r)\varphi B_{\mu\nu}$	$Q_{\varphi l}^{(3)}$	$(\varphi^\dagger i\overleftrightarrow{D}^I_\mu\varphi)(\bar l_p\tau^I\gamma^\mu l_r)$
$Q_{\varphi W}$	$\varphi^\dagger\varphi\, W^I_{\mu\nu}W^{I\mu\nu}$	Q_{uG}	$(\bar q_p\sigma^{\mu\nu}T^A u_r)\widetilde\varphi\, G^A_{\mu\nu}$	$Q_{\varphi e}$	$(\varphi^\dagger i\overleftrightarrow{D}_\mu\varphi)(\bar e_p\gamma^\mu e_r)$
$Q_{\varphi\widetilde W}$	$\varphi^\dagger\varphi\, \widetilde W^I_{\mu\nu}W^{I\mu\nu}$	Q_{uW}	$(\bar q_p\sigma^{\mu\nu}u_r)\tau^I\widetilde\varphi\, W^I_{\mu\nu}$	$Q_{\varphi q}^{(1)}$	$(\varphi^\dagger i\overleftrightarrow{D}_\mu\varphi)(\bar q_p\gamma^\mu q_r)$
$Q_{\varphi B}$	$\varphi^\dagger\varphi\, B_{\mu\nu}B^{\mu\nu}$	Q_{uB}	$(\bar q_p\sigma^{\mu\nu}u_r)\widetilde\varphi\, B_{\mu\nu}$	$Q_{\varphi q}^{(3)}$	$(\varphi^\dagger i\overleftrightarrow{D}^I_\mu\varphi)(\bar q_p\tau^I\gamma^\mu q_r)$
$Q_{\varphi\widetilde B}$	$\varphi^\dagger\varphi\, \widetilde B_{\mu\nu}B^{\mu\nu}$	Q_{dG}	$(\bar q_p\sigma^{\mu\nu}T^A d_r)\varphi\, G^A_{\mu\nu}$	$Q_{\varphi u}$	$(\varphi^\dagger i\overleftrightarrow{D}_\mu\varphi)(\bar u_p\gamma^\mu u_r)$
$Q_{\varphi WB}$	$\varphi^\dagger\tau^I\varphi\, W^I_{\mu\nu}B^{\mu\nu}$	Q_{dW}	$(\bar q_p\sigma^{\mu\nu}d_r)\tau^I\varphi\, W^I_{\mu\nu}$	$Q_{\varphi d}$	$(\varphi^\dagger i\overleftrightarrow{D}_\mu\varphi)(\bar d_p\gamma^\mu d_r)$
$Q_{\varphi\widetilde WB}$	$\varphi^\dagger\tau^I\varphi\, \widetilde W^I_{\mu\nu}B^{\mu\nu}$	Q_{dB}	$(\bar q_p\sigma^{\mu\nu}d_r)\varphi\, B_{\mu\nu}$	$Q_{\varphi ud}$	$i(\widetilde\varphi^\dagger D_\mu\varphi)(\bar u_p\gamma^\mu d_r)$

$(\bar LL)(\bar LL)$		$(\bar RR)(\bar RR)$		$(\bar LL)(\bar RR)$	
Q_{ll}	$(\bar l_p\gamma_\mu l_r)(\bar l_s\gamma^\mu l_t)$	Q_{ee}	$(\bar e_p\gamma_\mu e_r)(\bar e_s\gamma^\mu e_t)$	Q_{le}	$(\bar l_p\gamma_\mu l_r)(\bar e_s\gamma^\mu e_t)$
$Q_{qq}^{(1)}$	$(\bar q_p\gamma_\mu q_r)(\bar q_s\gamma^\mu q_t)$	Q_{uu}	$(\bar u_p\gamma_\mu u_r)(\bar u_s\gamma^\mu u_t)$	Q_{lu}	$(\bar l_p\gamma_\mu l_r)(\bar u_s\gamma^\mu u_t)$
$Q_{qq}^{(3)}$	$(\bar q_p\gamma_\mu\tau^I q_r)(\bar q_s\gamma^\mu\tau^I q_t)$	Q_{dd}	$(\bar d_p\gamma_\mu d_r)(\bar d_s\gamma^\mu d_t)$	Q_{ld}	$(\bar l_p\gamma_\mu l_r)(\bar d_s\gamma^\mu d_t)$
$Q_{lq}^{(1)}$	$(\bar l_p\gamma_\mu l_r)(\bar q_s\gamma^\mu q_t)$	Q_{eu}	$(\bar e_p\gamma_\mu e_r)(\bar u_s\gamma^\mu u_t)$	Q_{qe}	$(\bar q_p\gamma_\mu q_r)(\bar e_s\gamma^\mu e_t)$
$Q_{lq}^{(3)}$	$(\bar l_p\gamma_\mu\tau^I l_r)(\bar q_s\gamma^\mu\tau^I q_t)$	Q_{ed}	$(\bar e_p\gamma_\mu e_r)(\bar d_s\gamma^\mu d_t)$	$Q_{qu}^{(1)}$	$(\bar q_p\gamma_\mu q_r)(\bar u_s\gamma^\mu u_t)$
		$Q_{ud}^{(1)}$	$(\bar u_p\gamma_\mu u_r)(\bar d_s\gamma^\mu d_t)$	$Q_{qu}^{(8)}$	$(\bar q_p\gamma_\mu T^A q_r)(\bar u_s\gamma^\mu T^A u_t)$
		$Q_{ud}^{(8)}$	$(\bar u_p\gamma_\mu T^A u_r)(\bar d_s\gamma^\mu T^A d_t)$	$Q_{qd}^{(1)}$	$(\bar q_p\gamma_\mu q_r)(\bar d_s\gamma^\mu d_t)$
				$Q_{qd}^{(8)}$	$(\bar q_p\gamma_\mu T^A q_r)(\bar d_s\gamma^\mu T^A d_t)$

$(\bar LR)(\bar RL)$ and $(\bar LR)(\bar LR)$		B-violating	
Q_{ledq}	$(\bar l_p^j e_r)(\bar d_s q_t^j)$	Q_{duq}	$\varepsilon^{\alpha\beta\gamma}\varepsilon_{jk}\left[(d^\alpha_p)^T C u^\beta_r\right]\left[(q^{\gamma j}_s)^T C l^k_t\right]$
$Q_{quqd}^{(1)}$	$(\bar q_p^j u_r)\varepsilon_{jk}(\bar q_s^k d_t)$	Q_{qqu}	$\varepsilon^{\alpha\beta\gamma}\varepsilon_{jk}\left[(q^{\alpha j}_p)^T C q^{\beta k}_r\right]\left[(u^\gamma_s)^T C e_t\right]$
$Q_{quqd}^{(8)}$	$(\bar q_p^j T^A u_r)\varepsilon_{jk}(\bar q_s^k T^A d_t)$	Q_{qqq}	$\varepsilon^{\alpha\beta\gamma}\varepsilon_{jn}\varepsilon_{km}\left[(q^{\alpha j}_p)^T C q^{\beta k}_r\right]\left[(q^{\gamma m}_s)^T C l^n_t\right]$
$Q_{lequ}^{(1)}$	$(\bar l_p^j e_r)\varepsilon_{jk}(\bar q_s^k u_t)$	Q_{duu}	$\varepsilon^{\alpha\beta\gamma}\left[(d^\alpha_p)^T C u^\beta_r\right]\left[(u^\gamma_s)^T C e_t\right]$
$Q_{lequ}^{(3)}$	$(\bar l_p^j\sigma_{\mu\nu}e_r)\varepsilon_{jk}(\bar q_s^k\sigma^{\mu\nu}u_t)$		

Dim-6 operators

SMEFT cross sections

- Complete and independent dim-6 basis known: 2499 baryon conserving operators for 3 fermion generations; (can reduce assuming MFV, etc. to O(100))

Structure of a SMEFT cross section:

$$\boxed{\sigma \sim |\mathcal{M}_{SM}|^2 + \frac{1}{\Lambda^2} 2\text{Re}\left[\mathcal{M}_6 \mathcal{M}_{SM}^*\right] + \frac{1}{\Lambda^4}\left\{|\mathcal{M}_6|^2 + 2\text{Re}\left[\mathcal{M}_8 \mathcal{M}_{SM}^*\right]\right\}}$$

Leading SMEFT correction

Sub-leading; neglected in many analyses, including this talk

Semi-leptonic four-fermion operators

- Focus here on semi-leptonic four-fermion operators, relevant for both Drell-Yan at the LHC and DIS an the EIC

$\ell\ell qq$
$O_{\ell q}^{(1)} = (\bar{\ell}\gamma_\mu \ell)(\bar{q}\gamma^\mu q)$
$O_{\ell q}^{(3)} = (\bar{\ell}\gamma_\mu \tau^I \ell)(\bar{q}\gamma^\mu \tau^I q)$
$O_{eu} = (\bar{e}\gamma_\mu e)(\bar{u}\gamma^\mu u)$
$O_{ed} = (\bar{e}\gamma_\mu e)(\bar{d}\gamma^\mu d)$
$O_{\ell u} = (\bar{\ell}\gamma_\mu \ell)(\bar{u}\gamma^\mu u)$
$O_{\ell d} = (\bar{\ell}\gamma_\mu \ell)(\bar{d}\gamma^\mu d)$
$O_{qe} = (\bar{q}\gamma_\mu q)(\bar{e}\gamma^\mu e)$

l,q=left-handed doublets

e,u,d=right-handed singlets

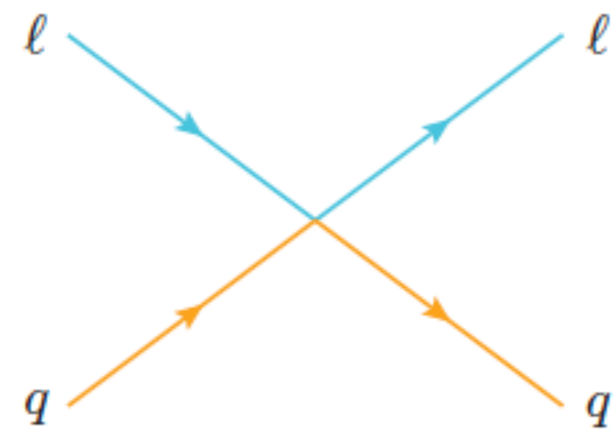

$$i[\gamma_\mu][\gamma^\mu]g_{11}^{(\ell q)} + i[\gamma_\mu][\gamma^\mu\gamma_5]g_{15}^{(\ell q)}$$
$$+ i[\gamma_\mu\gamma_5][\gamma^\mu]g_{51}^{(\ell q)} + i[\gamma_\mu\gamma_5][\gamma^\mu\gamma_5]g_{55}^{(\ell q)}$$

$$\begin{aligned}
g_{11}^{(eu)} &= \tfrac{1}{4}[C_{eu} + (C_{\ell q}^{(1)} - C_{\ell q}^{(3)}) + C_{\ell u} + C_{qe}] \\
g_{15}^{(eu)} &= \tfrac{1}{4}[C_{eu} - (C_{\ell q}^{(1)} - C_{\ell q}^{(3)}) + C_{\ell u} - C_{qe}] \\
g_{51}^{(eu)} &= \tfrac{1}{4}[C_{eu} - (C_{\ell q}^{(1)} - C_{\ell q}^{(3)}) - C_{\ell u} + C_{qe}] \\
g_{55}^{(eu)} &= \tfrac{1}{4}[C_{eu} + (C_{\ell q}^{(1)} - C_{\ell q}^{(3)}) - C_{\ell u} - C_{qe}]
\end{aligned}$$

Can transform the SMEFT basis to vector and axial couplings

LEP constraints

- Other operators contribute as well, and shift the ffV vertices

$$O_{\varphi\ell}^{(1)} = (\varphi^\dagger i \overleftrightarrow{D}_\mu \varphi)(\bar{\ell}\gamma^\mu \ell)$$

$$O_{\varphi\ell}^{(3)} = (\varphi^\dagger i \overleftrightarrow{D}_\mu \tau^I \varphi)(\bar{\ell}\gamma^\mu \tau^I \ell)$$

$$O_{\varphi e} = (\varphi^\dagger i \overleftrightarrow{D}_\mu \varphi)(\bar{e}\gamma^\mu e)$$

$$O_{\varphi q}^{(1)} = (\varphi^\dagger i \overleftrightarrow{D}_\mu \varphi)(\bar{q}\gamma^\mu q)$$

$$O_{\varphi q}^{(3)} = (\varphi^\dagger i \overleftrightarrow{D}_\mu \tau^I \varphi)(\bar{q}\gamma^\mu \tau^I q)$$

$$O_{\varphi u} = (\varphi^\dagger i \overleftrightarrow{D}_\mu \varphi)(\bar{u}\gamma^\mu u)$$

$$O_{\varphi d} = (\varphi^\dagger i \overleftrightarrow{D}_\mu \varphi)(\bar{d}\gamma^\mu d)$$

Dawson, Giardino 1909.02000

C_k	95% CL, $\Lambda = 1$ TeV
$C_{\varphi\ell}^{(1)}$	$[-0.043, 0.012]$
$C_{\varphi\ell}^{(3)}$	$[-0.012, 0.0029]$
$C_{\varphi e}$	$[-0.013, 0.0094]$
$C_{\varphi q}^{(1)}$	$[-0.027, 0.043]$
$C_{\varphi q}^{(3)}$	$[-0.011, 0.014]$
$C_{\varphi u}$	$[-0.072, 0.091]$
$C_{\varphi d}$	$[-0.16, 0.060]$
$C_{\varphi WB}$	$[-0.0088, 0.0013]$

These are strongly constrained by the precision Z-pole data of LEP, SLC; however, these experiments only weakly constrain four-fermion operators

Falkowski et al, 1706.03783

Blind spots at the LHC

- Goal: use LHC Drell-Yan data to derive quantitative constraints on qqll operators, to guide future experimental searches and model-building efforts
- But, LHC Drell-Yan is blind to certain combinations of coefficients. This is due to the observables measured, not the amount of integrated luminosity (more on this later).

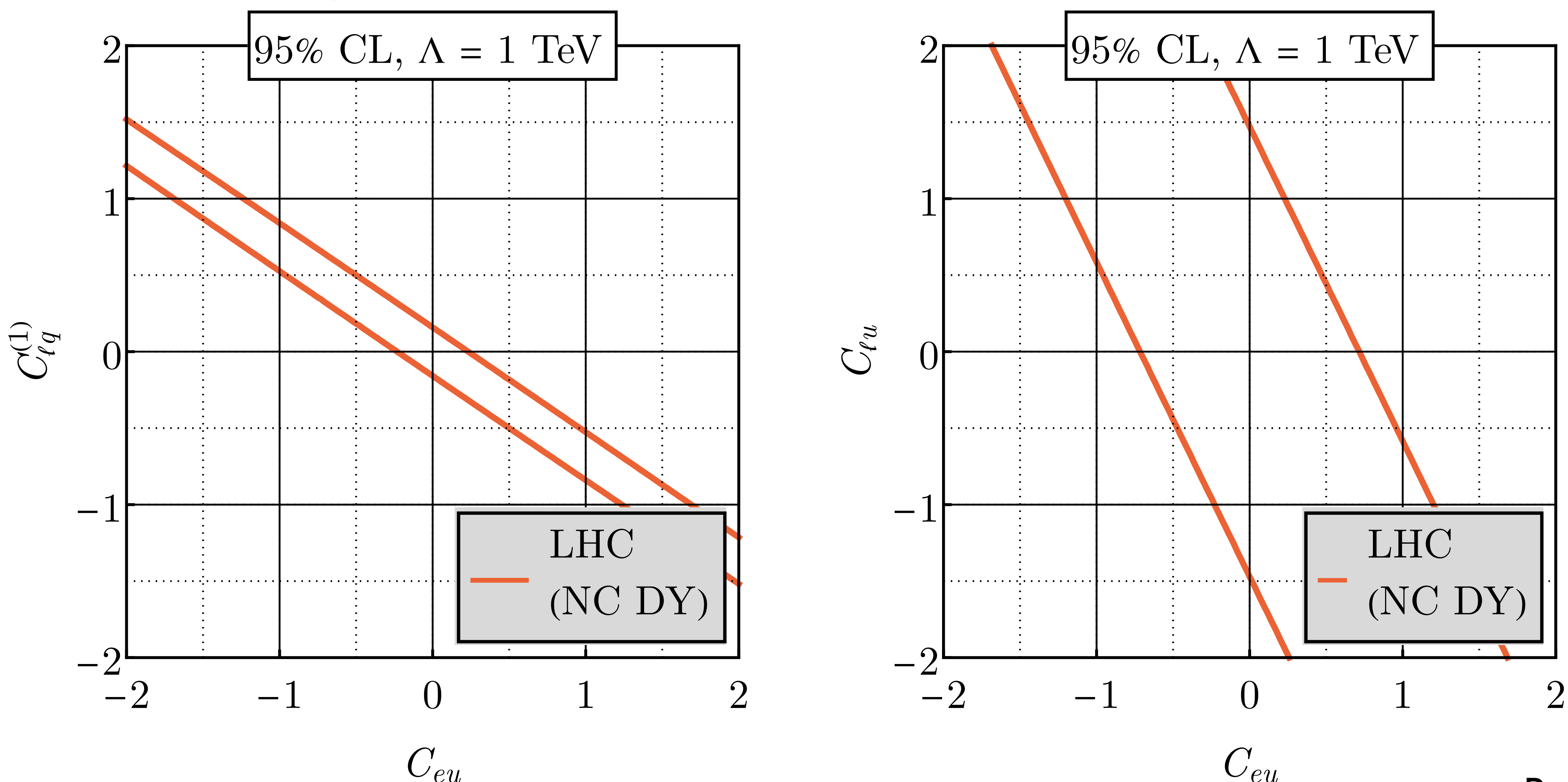

Regions inside red bands allowed with LHC data

Boughezal, FP, Wiegand
2004.00748

Blind spots at the LHC

- Goal: use LHC Drell-Yan data to derive quantitative constraints on qqll operators, to guide future experimental searches and model-building efforts
- But, LHC Drell-Yan is blind to certain combinations of coefficients. This is due to the ... ity (more on thi...

The EIC, with the possibility of polarizing both beams and therefore constructing more observables, doesn't suffer from these blind spots. Excellent opportunity for complementarity between the EIC and the LHC!

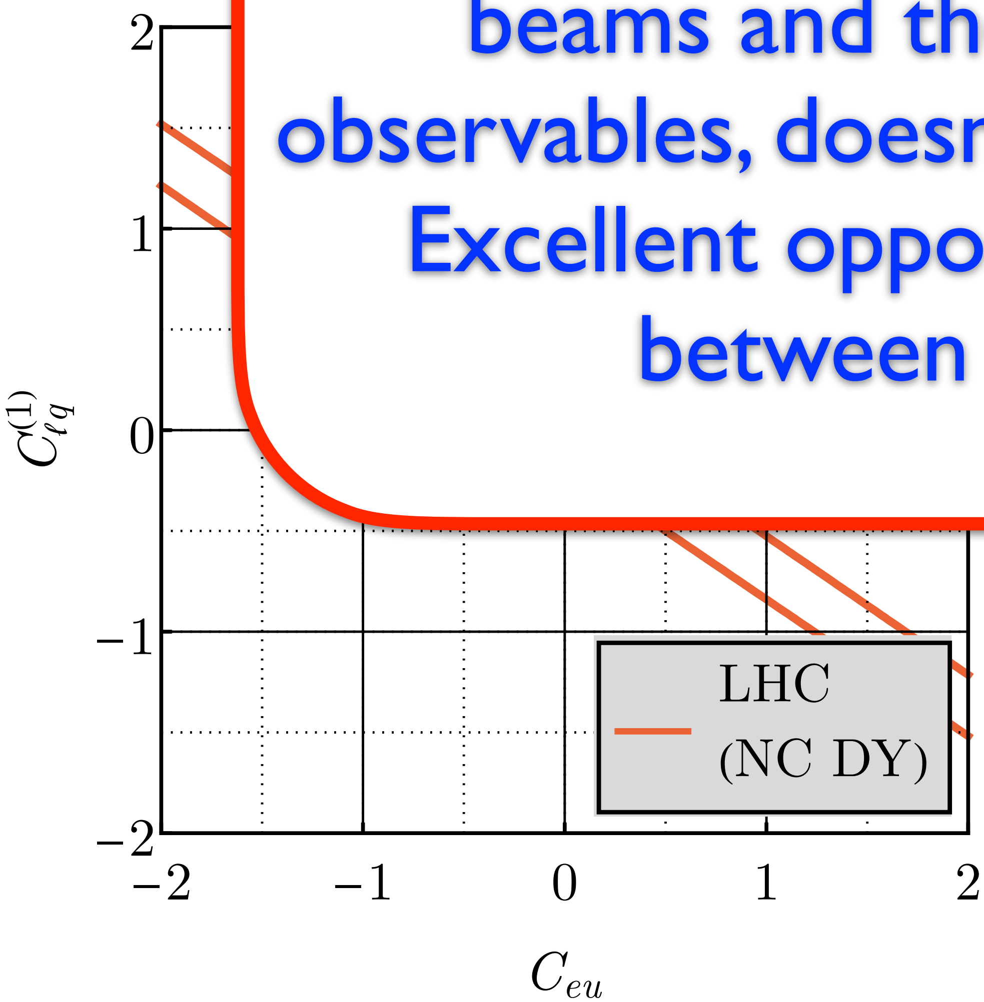

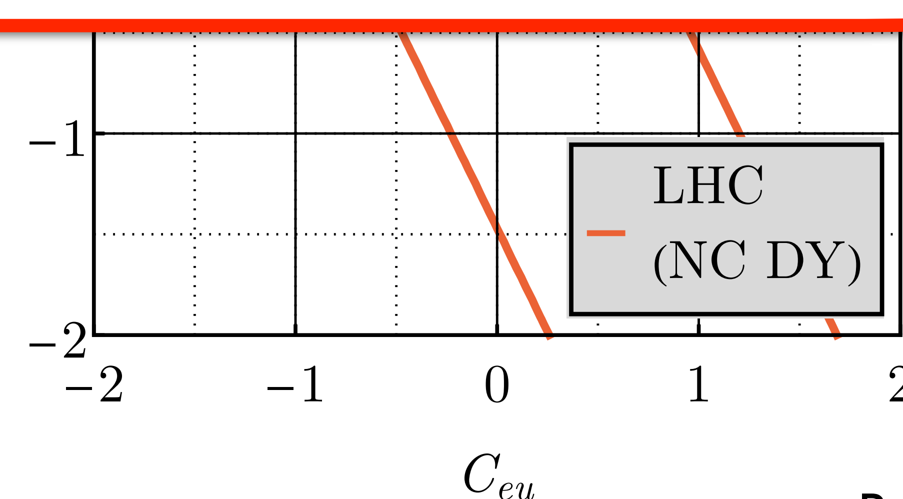

...ns inside red ... allowed with ... LHC data

Boughezal, FP, Wiegand
2004.00748

DIS at the EIC

- Let's look at the interference of the SMEFT operators with the SM for the up-quark channel in DIS, for arbitrary polarization of both beams.

$$\boxed{\begin{aligned}\frac{d^2\sigma_u^{\gamma SMEFT}}{dx dQ^2} \;=\; & -x\frac{Q_u Q^2}{8\pi\alpha}\Big[C_{eu}(1+\lambda_u)(1+\lambda_e)+(C_{lq}^{(1)}-C_{lq}^{(3)})(1-\lambda_u)(1-\lambda_e) \\ & +(1-y)^2 C_{lu}(1+\lambda_u)(1-\lambda_e)+(1-y)^2 C_{qe}(1-\lambda_u)(1+\lambda_e)\Big]\end{aligned}}$$

- We can form the following asymmetries:
  - Polarized electrons, unpolarized hadrons: $A_{\rm PV} = \frac{d\sigma_\ell}{d\sigma_0}$
  - unpolarized electrons, polarized hadrons: $\Delta A_{\rm PV} = \frac{d\sigma_H}{d\sigma_0}$
  - lepton charge asymmetries: $A_{\rm LC} = \frac{d\sigma_0(e^+H) - d\sigma_0(e^-H)}{d\sigma_0(e^+H) + d\sigma_0(e^-H)}$

Together with the y-dependence of the result, enough to disentangle all Wilson coefficients

Details of simulation

- We generate EIC pseudodata with the following effects included
  - Smearing, bin migration unfolding accounted for (details: 2204.07557)
  - Assume 80% electron, 70% proton/deuteron polarization
  - Inelasticity cuts: $y>0.1$, $y<0.9$
  - $x<0.5$, $Q>10$ GeV to avoid uncertainties from non-perturbative QCD and nuclear dynamics
- "Theory-only" simulation without any smearing, bin migration or unfolding reproduces the SMEFT sensitivities at the 20-30% level

Data sets

- We consider the following data sets that span the spectrum of possible EIC beam configurations

Deuteron			Proton	
D1	5 GeV $\times$ 41 GeV eD, 4.4 fb^{-1}		P1	5 GeV $\times$ 41 GeV ep, 4.4 fb^{-1}
D2	5 GeV $\times$ 100 GeV eD, 36.8 fb^{-1}		P2	5 GeV $\times$ 100 GeV ep, 36.8 fb^{-1}
D3	10 GeV $\times$ 100 GeV eD, 44.8 fb^{-1}		P3	10 GeV $\times$ 100 GeV ep, 44.8 fb^{-1}
D4	10 GeV $\times$ 137 GeV eD, 100 fb^{-1}		P4	10 GeV $\times$ 275 GeV ep, 100 fb^{-1}
D5	18 GeV $\times$ 137 GeV eD, 15.4 fb^{-1}		P5	18 GeV $\times$ 275 GeV ep, 15.4 fb^{-1}
			P6	18 GeV $\times$ 275 GeV ep, 100 fb^{-1}

- Red data sets provide the most sensitive probes of the SMEFT.
- Polarized deuteron and proton copies of these data sets are also studied, and labeled as ΔD, ΔP
- We also consider a high-luminosity version with x10 integrated luminosity

Error budget: unpolarized protons

- Bins ordered in Q^2, x; HL is a proposed high-luminosity option with x10 nominal integrated luminosity

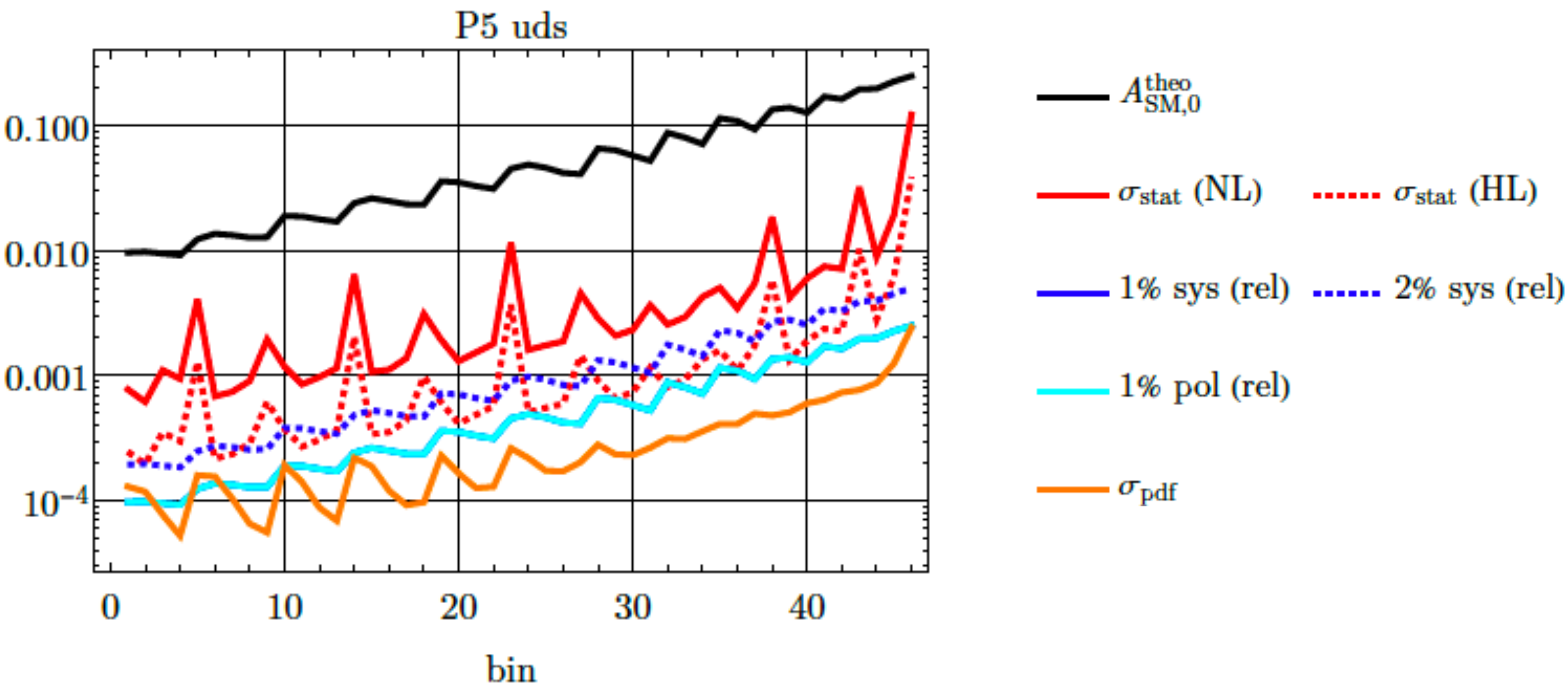

- Statistical uncertainties dominant with nominal luminosity; systematic errors more important with high luminosity; PDF errors negligible. Asymmetry much larger than all uncertainties.

Error budget: polarized protons

- Bins ordered in Q^2, x; HL is a proposed high-luminosity option with x10 nominal integrated luminosity

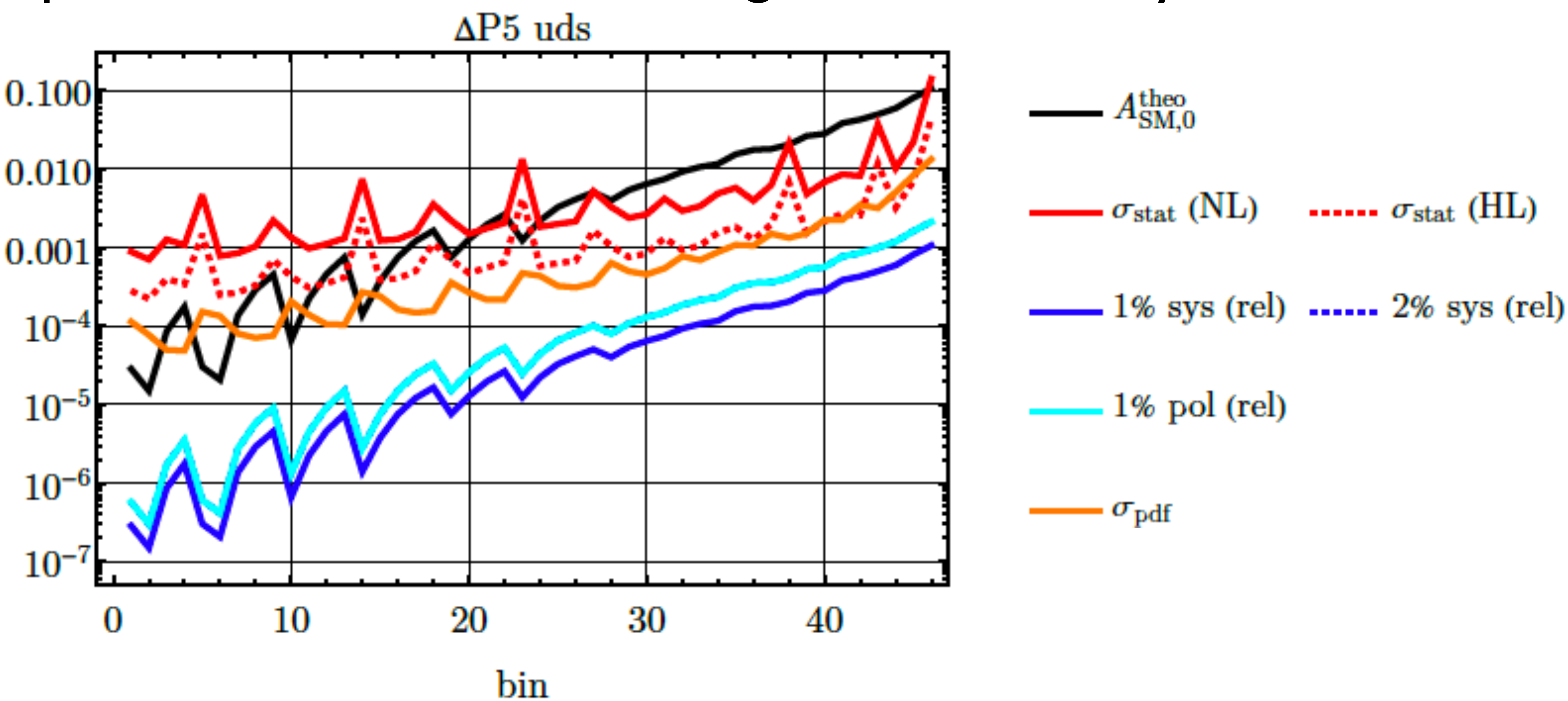

- Statistical uncertainties still dominant but PDF errors non-negligible, particularly with high luminosity option. Asymmetry only larger than statistical uncertainties in higher Q^2 bins.

SMEFT results: 1-d fits

- Consider the bounds on single Wilson coefficients first.

Boughezal et al, 2204.07557

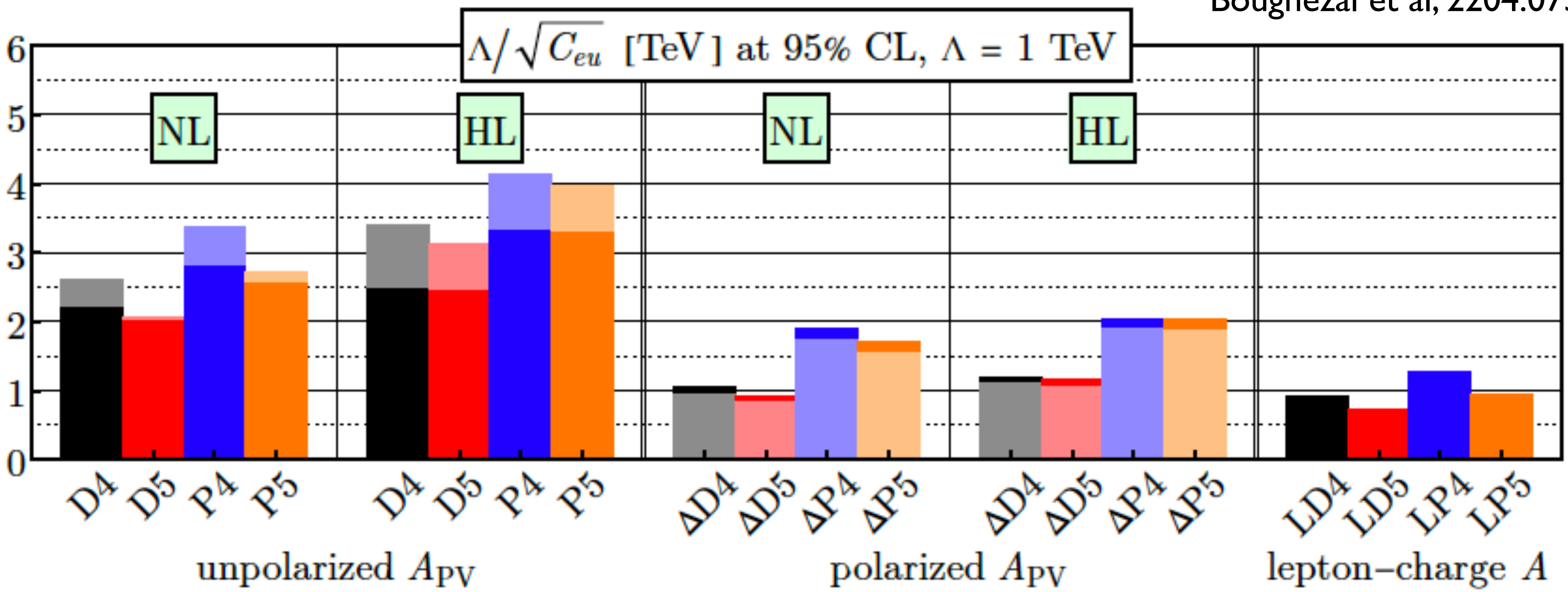

Trends:

- Proton sensitivities stronger than deuteron ones
- Unpolarized hadrons, polarized electrons offer strongest probes
- Lepton-charge asymmetries provide weakest probes

Pseudodata generation

$$A^{(e)}_{\text{pseudo},b} = A_{\text{SM},b} + r^{(e)}_b \sigma^{\text{unc}}_b + r'^{(e)} \sigma^{\text{cor}}_b$$

b=bin index

e=pseudo-experiment index (we average over numerous realizations of the EIC to remove fluctuations)

r_b, r'=random numbers in range [0,1]

uncorrelated errors; separate r_b for each bins

correlated errors; same r' for all bins

$$A_{\text{SMEFT},b} = \frac{\sigma^{(0)}_{\text{num},b} + \sum_{k=1}^{N_{\text{fit}}} C_k \sigma^{(1)}_{\text{num},b}}{\sigma^{(0)}_{\text{den},b} + \sum_{k=1}^{N_{\text{fit}}} C_k \sigma^{(1)}_{\text{den},b}}$$

Best-fit values:

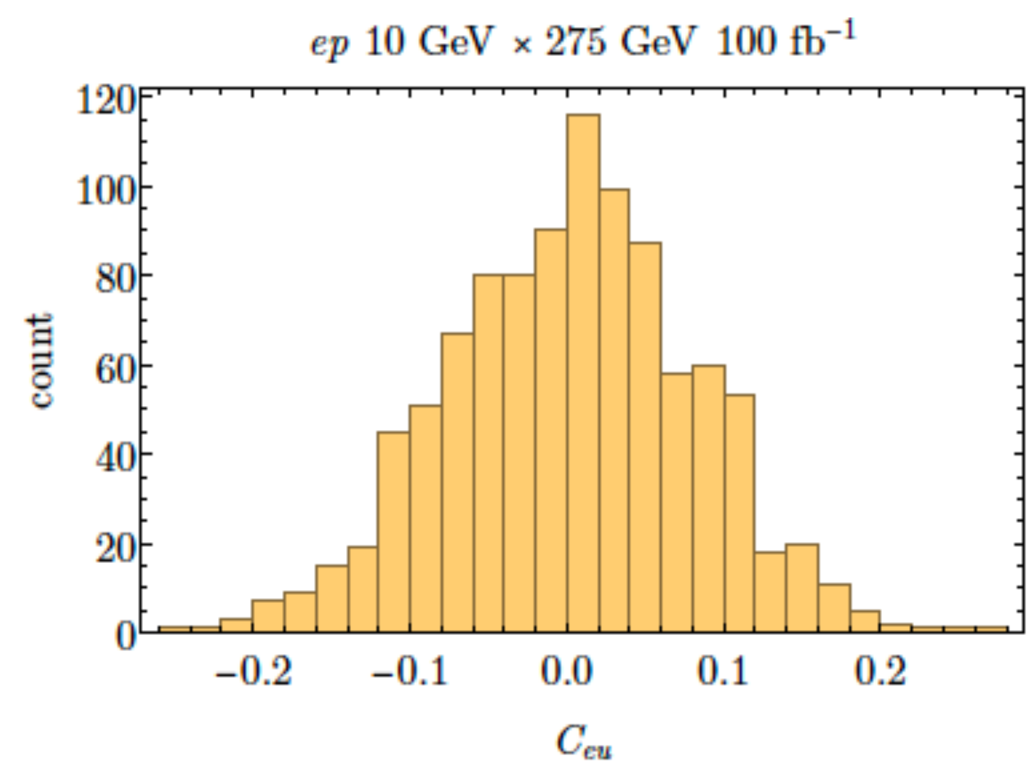

SMEFT results: 1-d fits

- Consider the bounds on single Wilson coefficients first.

Boughezal et al, 2204.07557

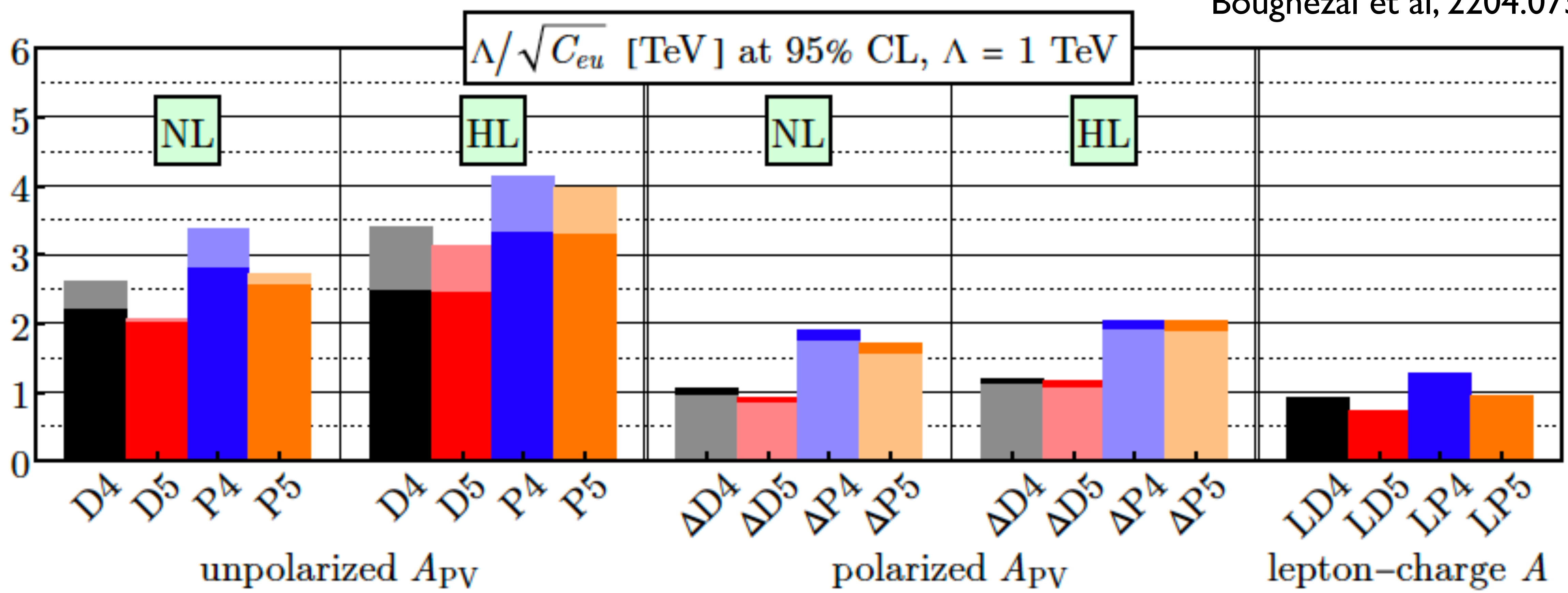

3 TeV scales probes with nominal luminosity, 4 TeV with high luminosity. Competitive with current LHC bounds.

SMEFT results: 2-d fits

- Can resolve the degeneracies that remain after LHC measurements! No degeneracies remain in the SMEFT parameter space with the nominal EIC luminosity.

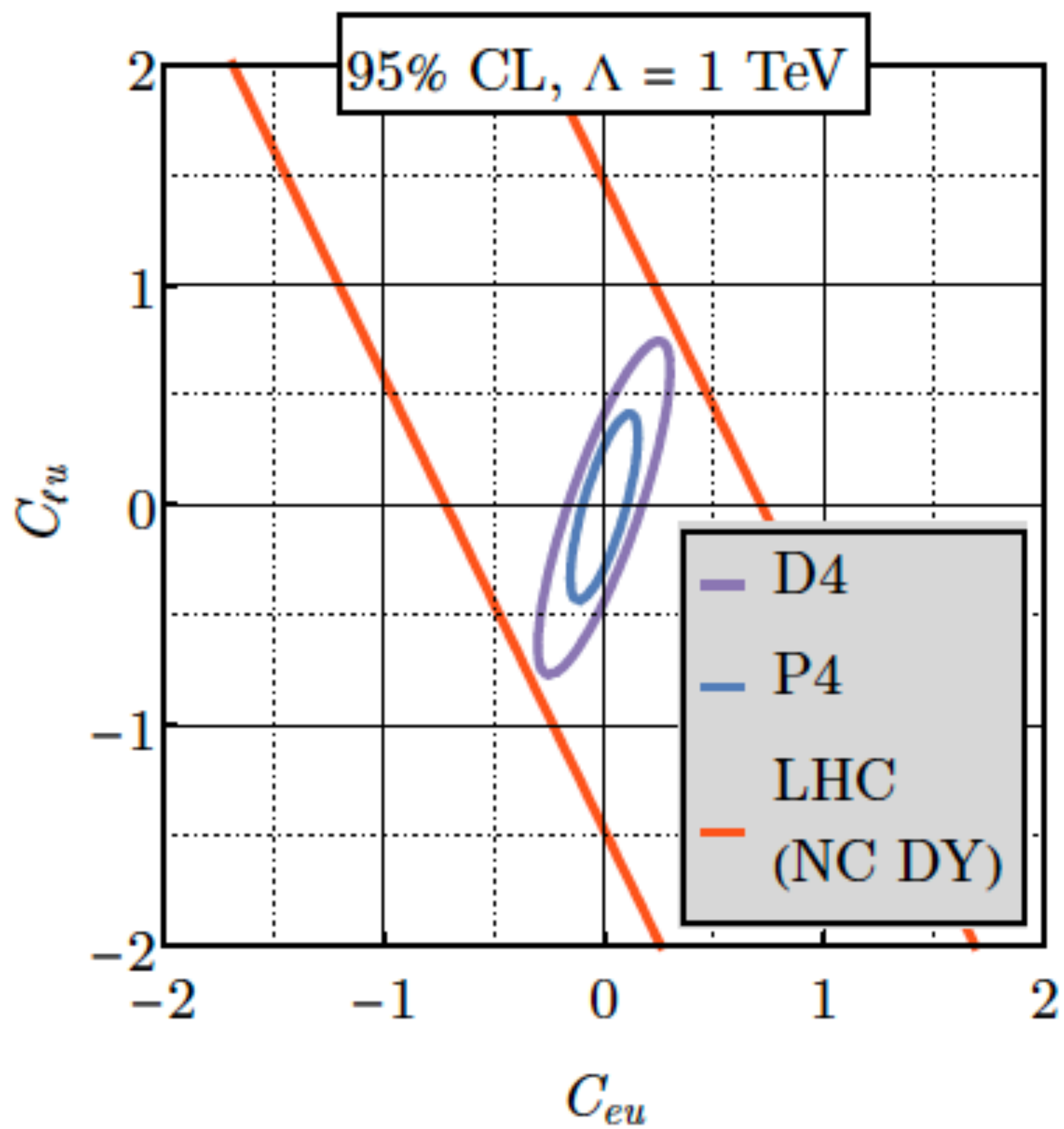

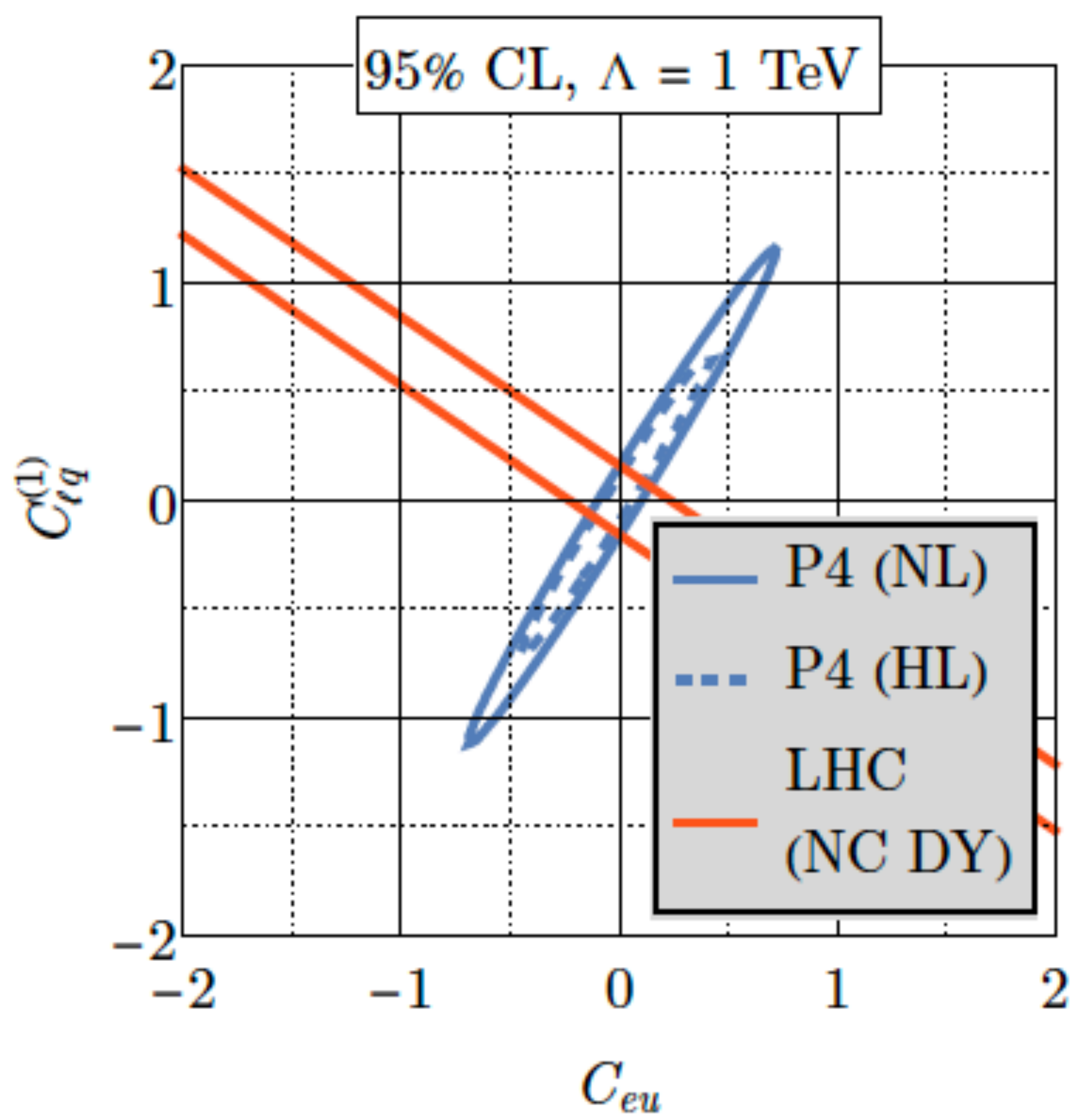

Boughezal et al, 2204.07557

Higher-dimensional fits

- Can turn on more Wilson coefficients to further search for degeneracies and check degradation of sensitivities. Requires more pseudo-experiments.

Boughezal et al, 2204.07557

N_{fit}	N_{exp}
2	10^3
3	10^4
4	10^5
5	10^6
6	10^7

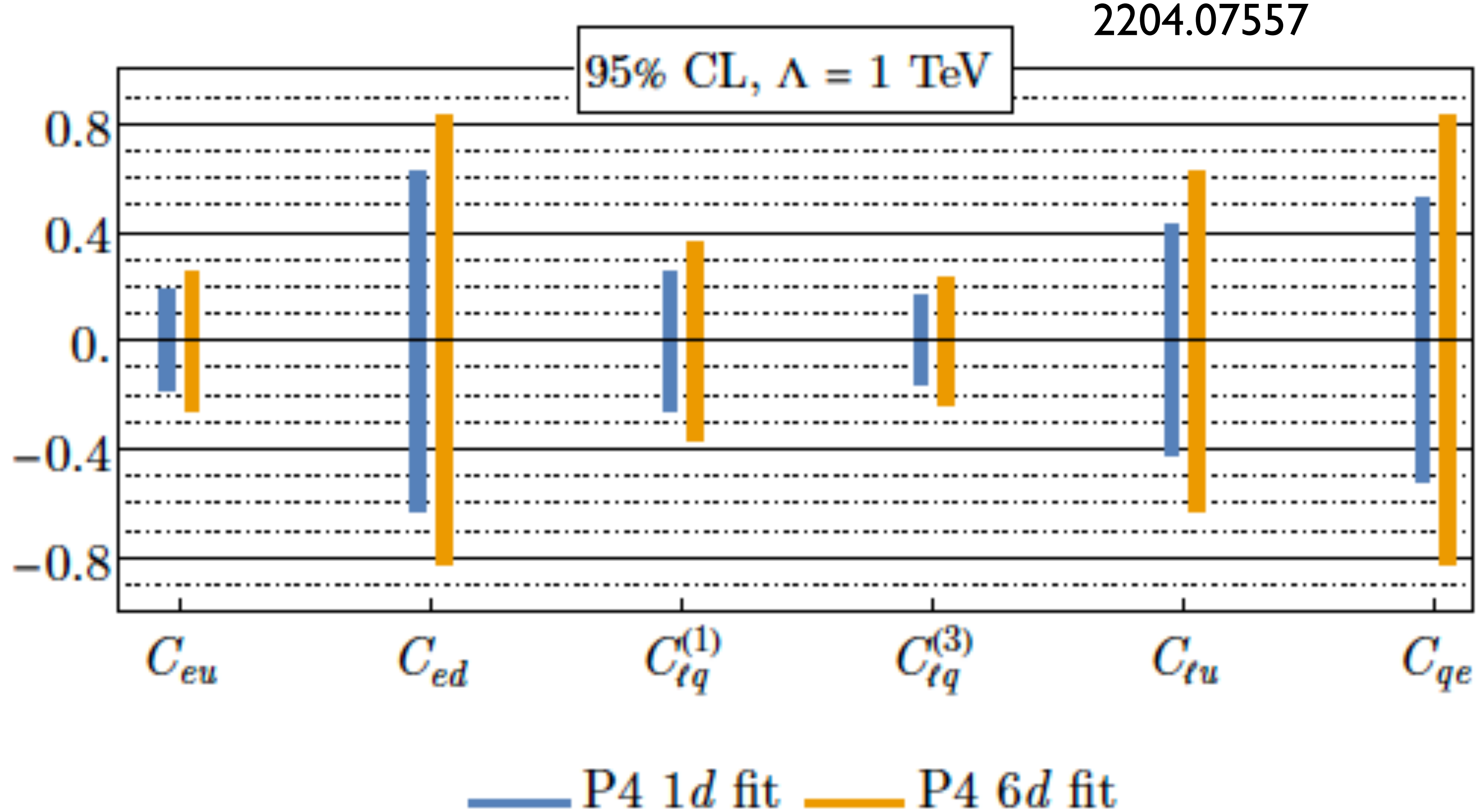

- No degeneracies in higher-d fits; only slightly weaker bounds. The EIC can probe the full 7-dimensional parameter space in this sector of the SMEFT.

Future LHC prospects

- The degeneracies at the LHC are due to the structure of the matrix elements, not the integrated luminosity. Limited room for improvement at the HL-LHC.

interference of photon diagram with SMEFT

Drell-Yan cross section in SMEFT:

red counts couplings, blue counts structures

$$\frac{d\hat{\sigma}^{\gamma SMEFT}_{u\bar{u}}}{dM^2 dY dc_\theta} = -\frac{8\pi\alpha Q_u}{3}\frac{\underbrace{(\overset{1}{C_{lu}} + \overset{2}{C_{qe}})\hat{t}^2}_{1} + \underbrace{(\overset{3}{C_{eu}} + \overset{4}{C^{(1)}_{lq}} - \overset{5}{C^{(3)}_{lq}})\hat{u}^2}_{2}}{\hat{s}},$$

$$\frac{d\hat{\sigma}^{ZSMEFT}_{u\bar{u}}}{dM^2 dY dc_\theta} = \frac{2g_Z^2}{3}\frac{\underbrace{(g^u_R g^e_L C_{lu} + g^e_R g^u_L C_{qe})\hat{t}^2}_{3} + \underbrace{(g^u_R g^e_R C_{eu} + g^u_L g^e_L C^{(1)}_{lq} - g^u_L g^e_L C^{(3)}_{lq})\hat{u}^2}_{4}}{\hat{s} - M_Z^2}$$

interference of Z diagram with SMEFT

Best case: in up-quark channel get four independent structures if we measure invariant mass and angle, for five SMEFT coefficients

Future LHC prospects

- The degeneracies at the LHC are due to the structure of the matrix elements, not the integrated luminosity. Limited room for improvement at the HL-LHC.

- In the high energy limit, $\hat{s} \gg M_Z^2$, we can no longer separately measure the SMEFT interferences with the photon and Z; both propagators become equivalent:

$$\frac{1}{\hat{s} - M_Z^2} \approx \frac{1}{\hat{s}}$$

- Can only measure two coupling structures, not four:

$$\boxed{\begin{array}{rl} -\frac{8\pi\alpha Q_u}{3}\left[(C_{lu} + C_{qe})\right] + \frac{2g_Z^2}{3}\left[g_R^u g_L^e C_{lu} + g_R^e g_L^u C_{qe}\right] & \hat{t}^2 \\ -\frac{8\pi\alpha Q_u}{3}\left[(C_{eu} + C_{lq}^{(1)} - C_{lq}^{(3)})\right] + \frac{2g_Z^2}{3}\left[g_R^u g_R^e C_{eu} + g_L^u g_L^e C_{lq}^{(1)} - g_L^u g_L^e C_{lq}^{(3)}\right] & \hat{u}^2 \end{array}}$$

Future LHC prospects

- The degeneracies at the LHC are due to the structure of the matrix elements, not the integrated luminosity. Limited room for improvement at the HL-LHC.

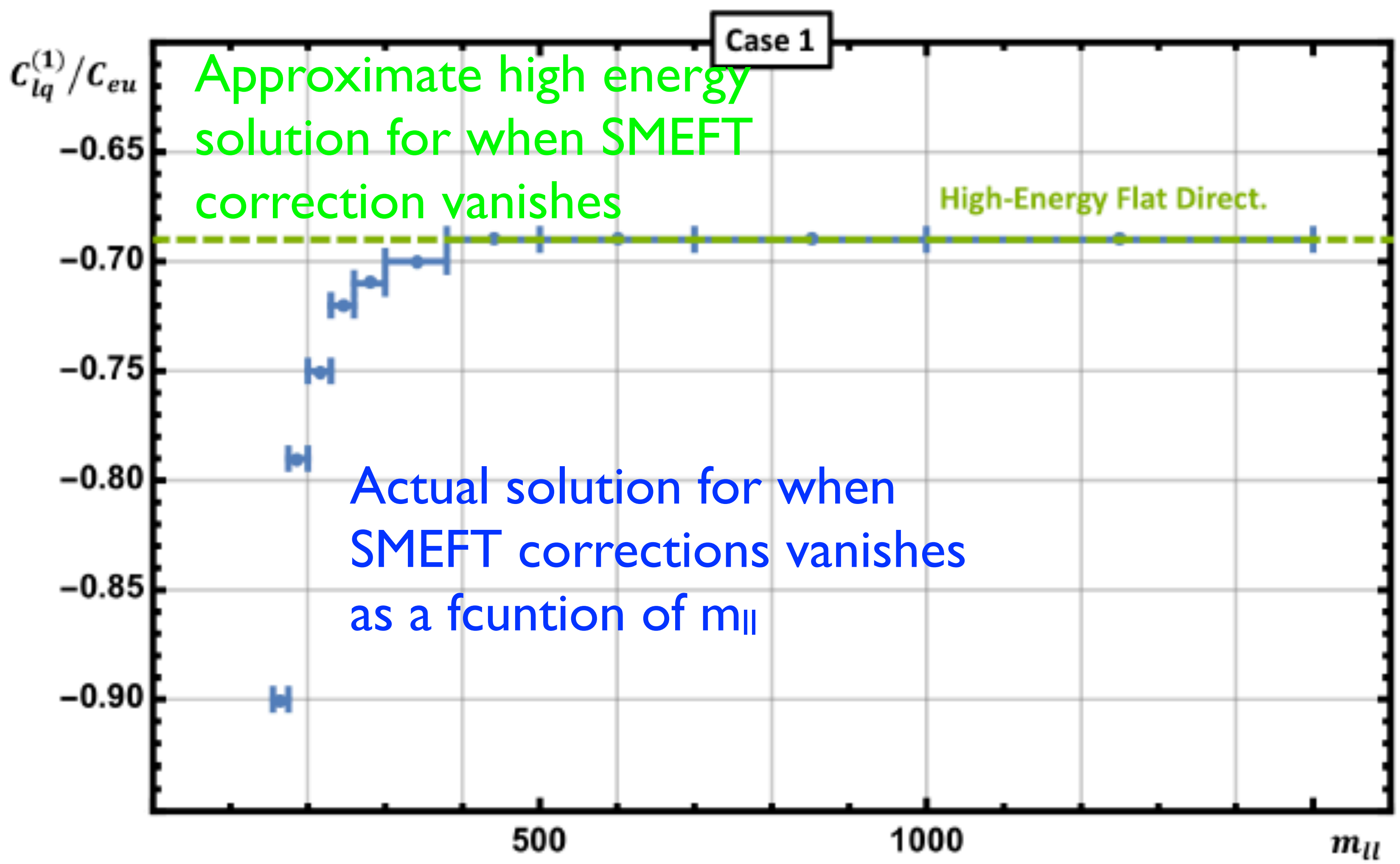

High energy limit almost exact by $m_{ll}\approx 300$ GeV; no advantage from the high energy of the LHC

Boughezal, FP, Wiegand 2004.00748

Future LHC prospects

- The degeneracies at the LHC are due to the structure of the matrix elements, not the integrated luminosity. Limited room for improvement at the HL-LHC.

Recall $\hat{t} = -\frac{\hat{s}}{2}(1 - c_\theta), \quad \hat{u} = -\frac{\hat{s}}{2}(1 + c_\theta)$

If the observable integrates over a symmetric range of cos(θ), LHC DY is only proportional to a *single* linear combination of couplings; many degeneracies in the parameter space for such observables! Most LHC measurements (invariant mass, transverse momentum, rapidity) fall in this category.

This is an ideal BSM science target for the EIC!

Conclusions

- The precision achievable at the EIC allows a wealth of important measurements, spanning QCD measurements to BSM searches
- In this talk we've reviewed the precision calculation of jet production at the EIC, and W-boson production at RHIC, and their applications to proton structure determinations.
- We've also pointed out that the EIC is capable of powerful probes of BSM effects difficult to access at the LHC due to its ability to polarize both beams.

Thanks for your attention!